Agricultural and Forest Meteorology 287 (2020) 107934

Contents lists available at ScienceDirect

Agricultural and Forest Meteorology

journal homepage: www.elsevier.com/locate/agrformet

Carbon, water and energy fluxes in agricultural systems of Australia and New Zealand

James Cleverly[a,b,*], Camilla Vote[c], Peter Isaac[d], Cacilia Ewenz[d,e], Mahrita Harahap[a], Jason Beringer[f], David I. Campbell[g], Edoardo Daly[h], Derek Eamus[a], Liang He[i], John Hunt[j], Peter Grace[k], Lindsay B. Hutley[l], Johannes Laubach[j], Malcolm McCaskill[m], David Rowlings[k], Susanna Rutledge Jonker[g,n], Louis A. Schipper[g], Ivan Schroder[o], Bertrand Teodosio[h], Qiang Yu[a,p,q], Phil R. Ward[r], Jeffrey P. Walker[h], John A. Webb[s], Samantha P.P. Grover[t]

[a] School of Life Sciences, University of Technology Sydney, Broadway, NSW, 2007, Australia
[b] Terrestrial Ecosystem Research Network, School of Life Sciences, University of Technology Sydney, Broadway, NSW, 2007, Australia
[c] Graham Centre for Agricultural Innovation, Charles Sturt University, Wagga, NSW, 2678, Australia
[d] TERN Ecosystem Processes/OzFlux central node, Melbourne, VIC 3159, Australia
[e] Airborne Research Australia, PO Box 335, Salisbury South, SA, 5106, Australia
[f] School of Agriculture and Environment, The University of Western Australia, Crawley, WA, 6020, Australia
[g] School of Science and Environmental Research Institute, University of Waikato, Private Bag 3105, Hamilton, New Zealand
[h] Department of Civil Engineering, Monash University, Clayton VIC 3800, Australia
[i] National Meteorological Center, Beijing 100081, China
[j] Manaaki Wenua-Landcare Research, P.O. Box 69040, Lincoln 7640, New Zealand
[k] Institute for Future Environments and Science and Engineering Faculty, Queensland University of Technology, Brisbane, QLD, 4000, Australia
[l] School of Environment, Research Institute for the Environment and Livelihoods, Charles Darwin University, NT, 0909, Australia
[m] Agriculture Victoria Research, 915 Mount Napier Rd, Department of Economic Development, Jobs, Transport and Resources, Hamilton, VIC 3300, Australia
[n] National Institute for Public Health and the Environment, Centre for Environmental Quality, PO Box 1, 3720 BA Bilthoven, the Netherlands
[o] International CCS & CO2CRC, Resources Division, Geoscience Australia, ACT, 2601, Australia
[p] State Key Laboratory of Soil Erosion and Dryland Farming on the Loess Plateau, Northwest A&F University, Yangling 712100, China
[q] College of Resources and Environment, University of Chinese Academy of Science, Beijing 100049, China
[r] CSIRO, Private Bag No 5, Wembley, WA, 6913, Australia
[s] Department of Ecology, Environment and Evolution, La Trobe University, Bundoora, VIC, Australia
[t] Applied Chemistry and Environmental Science, RMIT University, Melbourne VIC 3000, Australia

ARTICLE INFO

Keywords:
Wavelet-statistics conjunction
Eddy covariance
Precipitation pulses
Irrigation
Agriculture
Environmental variability

ABSTRACT

A comprehensive understanding of the effects of agricultural management on climate–crop interactions has yet to emerge. Using a novel wavelet–statistics conjunction approach, we analysed the synchronisation amongst fluxes (net ecosystem exchange NEE, evapotranspiration and sensible heat flux) and seven environmental factors (e.g., air temperature, soil water content) on 19 farm sites across Australia and New Zealand. Irrigation and fertilisation practices improved positive coupling between net ecosystem productivity (NEP = −NEE) and evapotranspiration, as hypothesised. Highly intense management tended to protect against heat stress, especially for irrigated crops in dry climates. By contrast, stress avoidance in the vegetation of tropical and hot desert climates was identified by reverse coupling between NEP and sensible heat flux (i.e., increases in NEP were synchronised with decreases in sensible heat flux). Some environmental factors were found to be under management control, whereas others were fixed as constraints at a given location. Irrigated crops in dry climates (e.g., maize, almonds) showed high predictability of fluxes given only knowledge of fluctuations in climate ($R^2 > 0.78$), and fluxes were nearly as predictable across strongly energy- or water-limited environments ($0.60 < R^2 < 0.89$). However, wavelet regression of environmental conditions on fluxes showed much smaller predictability in response to precipitation pulses ($0.15 < R^2 < 0.55$), where mowing or grazing affected crop phenology ($0.28 < R^2 < 0.59$), and where water and energy limitations were balanced (0.7 < net radiation / precipitation < 1.3; $0.27 < R^2 < 0.36$). By incorporating a temporal component to regression, wavelet–statistics conjunction provides an important step forward for understanding direct ecosystem responses to

* Corresponding author.
E-mail address: james.cleverly@uts.edu.au (J. Cleverly).

https://doi.org/10.1016/j.agrformet.2020.107934
Received 29 May 2019; Received in revised form 3 February 2020; Accepted 7 February 2020

environmental change, for modelling that understanding, and for quantifying nonstationary, nonlinear processes such as precipitation pulses, which have previously defied quantitative analysis.

1. Introduction

With the required expansion of agriculture necessary for feeding future populations, it is estimated that 10^9 ha of native and unmanaged ecosystems will be transformed into agricultural uses (Khan and Hanjra, 2009). The associated changes in land cover, land use, and thus ecosystem characteristics have well-established effects on the partitioning of energy and mass fluxes at the land surface. Shifts in albedo, physiology and mass and energy balances can affect weather patterns and regional climate as a result of changes in grazing, irrigation or biomass burning (Beringer et al., 2015, 2011; Jeong et al., 2014; Lara et al., 2017; Lynch et al., 2007; Mueller et al., 2017; Shao et al., 2017; Yang et al., 2017). As a consequence, biogeochemical cycles will likely be altered, including those of water, carbon, energy and nutrients (Beringer et al., 2011; Foley et al., 2005; Lara et al., 2017). Therefore, the transformation of unmanaged landscapes into managed agricultural systems (or vice-versa, as is sometimes the case with reforestation of previously cleared agricultural lands) will alter seasonal and annual biogeochemical cycles from local to global scales (Beringer et al., 2011; Cunningham et al., 2015).

Agricultural systems and yield are vulnerable to weather extremes and climate change (He et al., 2014a, 2018; Jin et al., 2017; Luo et al., 2018; Mallawaarachchi et al., 2017). Drought and heatwave present a risk of crop failure, although damage can be ameliorated through irrigation and associated evaporative cooling (Adamson et al., 2017; Dreccer et al., 2018; Ellis and Albrecht, 2017; Mueller et al., 2017; Rashid et al., 2018). However, too much precipitation can also present a great risk of crop failure, especially when extreme precipitation occurs aseasonally (Ellis and Albrecht, 2017). Between these extremes of droughts and flooding rains, mild water stress might not reduce productivity and yield, depending upon the selection and performance of drought-tolerant genotypes (Cai et al., 2017). Furthermore, climate change can have contrasting effects on winter and summer crops (Cammarano and Tian, 2018). There are strong regional differences in the responses of crops and ecosystems to climate (Dreccer et al., 2018; Hao et al., 2018; Raupach et al., 2013), particularly with respect to water- versus energy-limited ecosystems (Akuraju et al., 2017). These regional differences in environmental conditions inform the economic basis of agricultural management decisions (Meier et al., 2017; Regan et al., 2017). As such, there is an urgent need to identify how management practices across regions might affect the response of biogeochemical fluxes to climate and other environmental factors.

Agricultural management is intended to ameliorate unfavourable environmental conditions, thus management type and intensity can have a substantive effect on water and carbon dynamics (e.g., Behtari et al., 2019; Chi et al., 2016; Davis et al., 2010; Kirschbaum et al., 2017; Laubach et al., 2019; Moinet et al., 2019; Orgill et al., 2017; Ratcliffe et al., 2019; Schipper et al., 2019; Waters et al., 2017; Whitehead et al., 2018; Zeeman et al., 2010; Zhou et al., 2017). Moreover, water and carbon cycles of agricultural systems are complex, influenced heavily by location, soil type and management practises such as cultivar selection, tillage, fertiliser application, irrigation, crop rotation and management of residue and wastewater (Drewniak et al., 2015; Thompson et al., 1999; Waldo et al., 2016). Management practices affect soil carbon stocks in a multitude of ways, including through changes to primary productivity, biomass removal and decomposition (Kirschbaum et al., 2017; Whitehead et al., 2018). Agricultural management practices such as irrigation and grazing have direct and indirect effects on water-use efficiency (productivity / transpiration), evapotranspiration and CO_2 emissions (Kirschbaum et al., 2017; Tallec et al., 2013; Wagle et al., 2017a; Wang et al., 2017). In this study, the effects of management practices on productivity, evaporation and energy fluxes were investigated from across the agricultural sectors of Australia and New Zealand, ranging from grazed rangelands (low-intensity management) to irrigated/fertilised croplands and high-density dairy farms (high-intensity management).

Across Australia and New Zealand, *ca.* 52% of the landscape is managed at varying intensity for food and fibre production (Australian Bureau of Statistics, 2018; Statistics New Zealand, 2015). Agricultural ecosystems in Australia and New Zealand cover a vast range of climate and environmental conditions, from semiarid rangelands to the humid oceanic climate of New Zealand. Continuous measurements of fluxes and climate conditions across this range provides a wealth of information, but a method of statistical inference has yet to emerge which is not confounded by time-series measurements (Hargrove and Pickering, 1992; Murphy et al., 2010). Recently, wavelet-conjunction analysis has laid a firm theoretical framework for statistical inference of time series (Rhif et al., 2019); some examples are wavelet eigenvalue regression (Abry and Didier, 2018), wavelet principal components analysis (Cleverly et al., 2016a) and discrete wavelet multiple linear regression (Guan et al., 2015; He and Guan, 2013; He et al., 2014b). Building on this previous work, we used a novel wavelet–statistics conjunction to evaluate multivariate linear regression relationships between fluxes (net ecosystem exchange of carbon NEE, evapotranspiration E and sensible heat flux H) and environmental factors (e.g., air temperature T_a, specific humidity q, vapour pressure deficit D, soil water content θ, net radiation R_n, soil temperature T_s and ground heat flux G; see nomenclature for a list of factors and symbols). These environmental factors are not independent, thus our approach first included a wavelet–principal components analysis to identify dependencies amongst environmental factors and account for those interactions in subsequent regression analyses. Relationships between a flux and a principal component can be associated with the full suite of environmental conditions experienced at a site, as defined by the principal component or components which together explain a majority of the variability in a dataset. For example, if fluctuations in T_a and D were synchronised and thus both had large loadings in the same principal component, any relationship between a flux and that principal component during subsequent regression analysis would then be associated with coordinated fluctuations in both T_a and D, each in proportion to its dependence on the other. This proportion would then be related to each factor's relative, coordinated amplitude and phase (i.e., component loading in principal components analysis), the degree to which their principal component is related to a flux (from regression analysis), and the proportion of the variation which is explained by their principal component (i.e., the eigenvalue of the principal component). This study aims to synthesise the results from eddy covariance measurements in agricultural ecosystems across the OzFlux research network (http://ozflux.org.au; (Beringer et al., 2016)) of the Terrestrial Ecosystem Research Network (Cleverly et al., 2019) and additional independent sites to address the following research question:

How do fluxes under different types of management activities (grazed rangelands, dryland farming, irrigated agriculture, and high density grazing with large input requirements) differ in their responses to environmental drivers?

We hypothesised that: (i) coupling amongst fluxes was expected to be similar across sites within a level of management intensity (low, intermediate, high) because carbon and water fluxes will experience greater physiological coupling if management plays a role in

Nomenclature

Environmental factors

ϕ	short-term dryness index (-)
ρ_v	absolute humidity (g m^{-3})
θ	soil water content (m^3 m^{-3})
D	vapour pressure deficit (kPa)
G	ground heat flux (W m^{-2}), (MJ m^{-2} d^{-1})
P	precipitation (mm d^{-1})
q	specific humidity (g^{-1})
R_n	net radiation (W m^{-2}), (MJ m^{-2} d^{-1})
T_a	air temperature (°C)
T_s	soil surface temperature (°C)

Turbulent fluxes

BR	Bowen ratio (-)
E	evapotranspiration (mm d^{-1})
H	sensible heat flux (W m^{-2}), (MJ m^{-2} d^{-1})
NEE	net ecosystem exchange of carbon (μmol m^{-2} s^{-1}), (gC m^{-2} d^{-1})
−NEE	net ecosystem productivity (μmol m^{-2} s^{-1}), (gC m^{-2} d^{-1})

Wavelets

Ψ	mother wavelet
a_{max}	timescale of peak coherence
CWT	continuous wavelet transform
DWT	discrete wavelet transform

Statistics

α_i	ith component loading
β_i	regression coefficient for the ith component
ε	regression model error
λ_i	ith eigenvalue
r^2	squared correlation, coherence
R^2	coefficient of determination
$envPC_i$	ith principal component for environmental factors
$fluxPC_i$	ith principal component for turbulent fluxes
wCCA	wavelet canonical correlation analysis
wMLR	wavelet multiple linear regression
wPCA	wavelet principal components analysis

ameliorating crop stress; (ii) coupling amongst environmental factors would be weakened by increasingly intense management, due to the divergence of local and regional climate under highly intense management; and (iii) relationships between fluxes and environmental factors would be similar within a level of management intensity (low, intermediate, high) as a result of hypotheses (i) and (ii). In this work, eddy covariance sites will be identified by their FLUXNET code (AU-xxx, NZ-xxx).

2. Agricultural sites description

Nineteen sites in Australia and New Zealand with uninterrupted time series of fluxes and environmental factors during at least one complete growing season were identified for analysis (Table 1, Fig. 1). Because uninterrupted time series are required for wavelet analysis, site selection was restricted to those which contained few, small gaps during the peak of the growing season. Agricultural ecosystems were classified by management intensity: low, intermediate and high. Due to restrictions on the distribution of eddy covariance sites, only one or two datasets sometimes exist for a given management practice (e.g., dryland food crops, $n = 1$), thus management intensity categories could not be further divided by specific management practice without losing statistical power and rigour. Management at low to negligible intensity included only Australian grazed rangelands, which are stocked at very low density and are absent of land clearing, irrigation and fertilisation. At the other extreme, sites with highly intense management have been cleared and levelled, although the regular receipt of irrigation and fertilisation was used to define the high-intensity management class, both for crops and for dairy pastures. Management practices at intermediate-intensity sites often included land clearing and nursery support (e.g., planting, initial but not continuing irrigation or fertilisation for promoting establishment only). Sites with moderate-intensity management included improved pasturelands and unirrigated (dryland) crops, either for consumption by people (food crops) or as forage for livestock (forage crops). Food crops are generally harvested at the end of the growing season, whereas forage crops are typically harvested repeatedly throughout the growing season. These 19 sites represent common agricultural activities across a wide range of regions and climates; see supplementary information S1 for a detailed description of the agricultural land use at each site.

To constrain the large range of regional variation across Australia and New Zealand, four sets of co-located sites were included in this study. The paired grazed-rangeland sites AU-ASM and AU-TTE were co-located on Pine Hill Cattle station in semiarid central Australia, where grazing pressure ranges from small in the woodland at AU-ASM (*Acacia* spp.) to negligible in the unpalatable hummock grasses of AU-TTE (*Triodia schinzii*). Measurements of three "paired" irrigated broadacre crops were co-located at relatively close proximity in the Coleambally irrigation area (AU-Cm1, AU-Cm2), where irrigation intensity was highest for rice (*Oryza sativa*), intermediate for summer-season maize (*Zea mays*, also known as corn in some parts of the world), and smallest for wheat (*Triticum sativa*) due to reduced evaporative demand in the winter. In both sets of paired sites in New Zealand, highly intense management in the form of irrigation and fertilisation was compared to intermediate-intensity management for livestock, either as a rainfed forage crop or an intermittently grazed pasture. One pair of sites was located on Beacon Farm, where the comparison was between irrigated and fertilised ryegrass (*Lolium perenne*) and clover (*Trifolium repens*) pasture versus rainfed kale (*Brassica oleracea*) (NZ-BFm and NZ-BFu, respectively; Laubach and Hunt, 2018). The second set of paired sites in NZ was at Ashley Dene farm, where the comparison was between an irrigated lucerne (*Medicago sativa*) crop (NZ-ADw), which is also known as alfalfa in some parts of the world, and a rainfed lucerne crop (NZ-ADn).

3. Methods

3.1. Measurements: eddy covariance and environmental conditions

Most of the eddy covariance sites across the OzFlux network use a standard set of instruments, although there is some variation due to site-specific limitations (Isaac et al., 2017). Detailed descriptions of sites, flux tower installation and instrumentation can be found in the references of Table 1. Each EC system was operated at a measurement frequency of 10 or 20 Hz, and fluxes were computed from covariance with vertical wind speed over a 30-min interval except at AU-Otw, where fluxes were computed hourly. Flux data were processed following Isaac et al. (2017). NEE was assumed to be equal to net carbon flux F_c, where NEE $= F_c = \overline{w'c'}$, w is vertical wind speed, c represents atmospheric carbon dioxide density, primes represent fluctuation

around the mean, and the overbar represents a temporal average. Similarly, H was determined as $H = \rho_a C_p \overline{w'T'_a}$, where ρ_a is air density and C_p is the specific heat of air. E was measured as a mass flux $E_{mass} = \overline{w'\rho'_v}/\rho_w$ and converted to a 30-min depth equivalent (i.e., converted to units of mm 30-min^{-1}), where ρ_v is absolute humidity and ρ_w is the density of water. Latent heat flux (LE) was determined as the product of L_v and E_{mass}, where L_v is the latent heat of vaporisation and was computed following Stull (1988) as a function of independently measured air temperature (Isaac et al., 2017). See Isaac et al. (2017) for a detailed description of quality control and post-processing procedures used in TERN OzFlux.

Because wavelet analysis requires uninterrupted time series, the potential for gapfilling bias is present. Biases introduced during gap filling were minimised by (i) selecting a short analysis period which avoids large gaps (61 days, see §3.2) and (ii) careful screening of each dataset for obvious errors introduced during gapfilling (e.g., vapour pressure deficit < 0). However, screening came with the potential expense of under-representing agricultural sites in areas of high farm density (cf. Figs. 1 and S1). Gapfilled flux datasets were obtained from http//data.ozflux.org or from individual sites. Local optimisation of gapfilling procedures is essential for minimising bias (Isaac et al., 2017), just as local site knowledge is key for providing confidence and consistency in statistical findings (van Gorsel et al., 2018). Wavelet–-statistics conjunction could provide a powerful tool for comparing gapfilling approaches (e.g., Moffat et al., 2007), although a complete evaluation of gapfilling procedures should not be limited to agricultural sites and is beyond the scope of the current study.

Gaps in fluxes (NEE, E, H) were filled using either a self-organising linear output (SOLO) model (Eamus et al., 2013; Isaac et al., 2017) or a feed-forward artificial neural network in DINGO (Dynamic INtegrated Gap-filling and partitioning for OzFlux; Beringer et al., 2017) following Moffat et al. (2007). SOLO is an artificial neural network which (Eamus et al., 2013; Hsu et al., 2002): (a) employs a linear statistical kernel, resulting in minimal errors due to over-training; (b) provides access to intermediate products (i.e., SOLO is not a black box type of artificial neural network); and (c) produces small root mean square errors when used for gap filling. Gaps in meteorology were filled using a variety of strategies depending on data availability and suitability, including: SOLO trained on environmental drivers from a paired tower (Cleverly et al., 2016c); linear interpolation for small gaps (≤ 60 min); regressions from ancillary data of automatic weather stations operated by the Bureau of Meteorology (in Australia); output from a numerical weather prediction model known as the Australian community climate Earth system simulator (ACCESS); output from the ERA-Interim reanalysis product; or vegetation indices from the moderate resolution imaging spectroradiometer (MODIS) satellite (Isaac et al., 2017). Eight of the datasets used in this study contained no gaps in measurements of environmental factors during the chosen analysis period. Gaps in environmental factors amounted to 0.08 ± 0.04% of observations across all sites, exclusive of the grazed rangeland AU-Stp where gaps in environmental factors amounted to 35% of the data during the chosen analysis period. Nonetheless, AU-Stp was retained in the analysis to maintain a minimum sample size of three grazed rangeland sites for analysis in this study.

4. Analysis periods

Analysis periods of 61 days were chosen to span the peak of the growing season, defined by consistently low (i.e., highly negative) values of daytime NEE, but also to minimise overlap with green-up or senescence periods. Data records for some sites were restricted to a single year, particularly for those from irrigated broadacre crops (AU-Cm1, AU-Cm2), thus a single growing season was chosen for evaluation of the 19 sites in the study. Measurements were collected in an anomalously wet year from AU-Cm1 and AU-Cm2, thus a growing season for sites with multi-year records was chosen as the most productive year in the record. Differences in climate across sites and years are important

Table 1
Site details, major land use/land cover and management intensity. L: low-intensity management. I: intermediate-intensity management. H: high-intensity management.

Site	Lat/Long	Elevation (m asl)	Dominant vegetation/Management Intensity	Major soil type	Temporal coverage	Reference
AU-TTE	−22.29, 133.64	600	Hummock grassland savanna (L)	Red kandasol, drainage sand	Est. 2012	Cleverly et al. (2016c)
AU-ASM	−22.28, 133.25	600	Mulga woodland savanna (L)	Red kandasol	Est. 2010	Cleverly et al. (2013); Eamus et al. (2013)
AU-Stp	−17.15, 133.35	228	Mitchell grassland (L)	Grey vertosol	Est. 2008	Hutley et al. (2011)
AU-Otw	−38.51, 142.80	52	Pasture (I)	Mottled sandy yellow (Sodosol)	2007–2011	Etheridge et al. (2011); Loh et al. (2009)
AU-DaP	−14.06, 131.32	75	Pasture (I)	Red kandasol	2007–2013	Hutley et al. (2011)
NZ-Oxf	−43.26, 172.21	235	Converted paddock (I)	Taitapu Typic Orthic Gley	2005–2010	Brown et al. (2009)
AU-Rig	−36.66, 145.58	152	Pasture (I)	Sodosol	Est. 2010	Beringer et al. (2016)
AU-Gat	−37.39, 141.96	255	Winter pasture (I)	Brown Chromosol/Sodosol	2015–2015	Dresel et al. (2018)
AU-Emr	−23.86, 148.48	170	Chick peas, wheat & pasture (I)	Grey vertosol	2011–2014	Berko et al. (2012)
AU-Sam	−27.39, 152.88	90	Improved pasture (I)	Redoxic hydrosol	Est. 2010	van Delden et al. (2016)
NZ-BFu	−43.59, 171.93	204	Kale (I)	Lismore silty loam	2012–2014	Hunt et al. (2016)
NZ-ADn	−43.65, 172.35	34	Lucerne (I)	Stony Balmoral silty loam	Est. 2015	Laubach et al. (2019)
AU-Lox	−34.47, 140.66	36	Almond orchard (H)	Mallee highland (Sodosol)	2008–2009	Stevens et al. (2012)
AU-Cm1	−34.76, 146.02	120	Broadacre crops (maize & wheat) (H)	Transitional red brown earth	2010–2011	Vote et al. (2015)
AU-Cm2	−34.93, 145.82	120	Broadacre crops (rice) (H)	Transitional red brown earth	2010–2011	Vote et al. (2015)
NZ-Sco	−37.77, 175.38	41	Pasture for dairying (H)	Matangi silt loam	Est. 2007	Mudge et al. (2011); Rutledge et al. (2015)
NZ-BFm	−43.59, 171.93	204	Pasture for dairying (H)	Lismore silty loam	2012–2015	Hunt et al. (2016)
NZ-ADw	−43.64, 172.35	33	Lucerne (H)	Stony Balmoral silty loam	Est. 2015	Laubach et al. (2019)

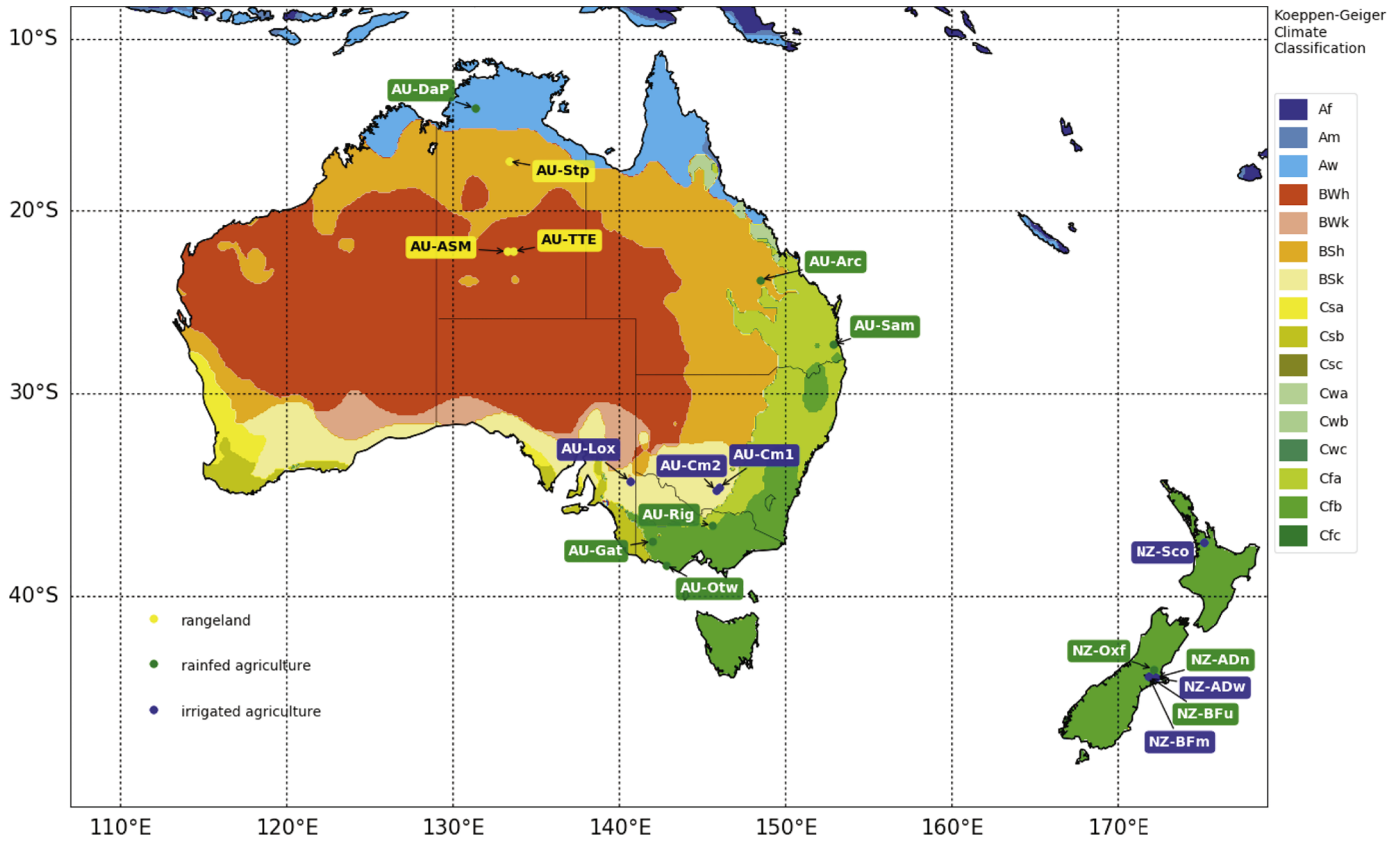

Fig. 1. Locations of TERN OzFlux sites used in the analysis and regional Köppen–Geiger climate zones. Sites are categorised by management intensity (rangeland, rainfed agriculture, irrigated agriculture).

confounding factors for comparisons across the network, and these issues cannot be ignored. However, a survey of agricultural management conducted from flux measurements collected simultaneously is impractical, thus we will interpret the results of this study under the conditions observed during the growing season under analysis (Table 2).

Many of the sites in this study provided a single season of flux data (Table 2), and this was often during a highly productive year like 2010–2011 in Australia (Boening et al., 2012; Cleverly et al., 2016a; Poulter et al., 2014; Xie et al., 2019). Thus to avoid confounding factors of interannual fluctuations in stress and productivity, comparisons in this study were made for each site during its most productive growing season (i.e., the growing season with the lowest daytime NEE). Whereas some sites were highly productive during wet conditions (e.g., irrigated broadacre crops AU-Cm1, AU-Cm2; grazed rangelands AU-ASM, AU-Stp), others were evaluated during drought, including the final year of the Millennium Drought (2009; improved pasture AU-Otw, irrigated almonds AU-Lox), ten years of hydrological drought which generated hardships for irrigated agriculture (Mallawaarachchi et al., 2017; van Dijk et al., 2013), and 2012–2013, the return of drought (improved pasture in the Northern Territory, AU-Dap; rainfed crops and improved pasture in Queensland, AU-Emr and AU-Sam). (Table 2). Climate has continued to fluctuate between extremes of droughts, heatwaves and flooding rains (Cleverly et al., 2016a, 2016c; Ma et al., 2016), creating much uncertainty in the agricultural sector (Ellis and Albrecht, 2017). The analysis period for AU-TTE was identified during the return of wet conditions in the summer of 2016–2017, when precipitation in the two months preceding the analysis window (546 mm, 17 Dec 2016–6 February 2017) was similar to that which fell across the entire water year 2010–2011 at AU-TTE's paired site, AU-ASM (565 mm, 1 September 2010–31 August 2011; Cleverly et al., 2016c) (Table 2).

Intense grazing events in New Zealand can strongly increase NEE through enhanced carbon emissions and removal of photosynthetic biomass (Hunt et al., 2016). Thus, analysis periods for flux measurements from New Zealand were either (i) around the peak of the growing season, when high growth rates kept NEE low despite the occurrence of defoliation episodes; or (ii) after conversion to forage crops such as kale (e.g., NZ-BFu).

As an indication of the short-term balance between energy and water limitations on NEE and E, an aridity index value (ϕ) was calculated as $\phi = R_n / (\rho_w L_v P)$ over the analysis period, where ρ_w is the density of water and P is precipitation. Caution is urged regarding the interpretation of ϕ in this study as a short-term measure of ϕ cannot be used to draw inferences of long-term aridity, hydrology or climatology, contrary to the original definition and use of ϕ at an annual timescale (Budyko, 1974). To further characterise site conditions, the Bowen ratio (BR) was also determined as $BR = H / LE$ over the same period.

5. Data analysis

A wavelet–statistics conjunction approach was used for all inferences in this study. Time series measurements are an extreme case of the repeated measures experimental design, representing many multiples of repeated observations on an individual experimental unit. This restriction on random sampling creates the possibility of auto-correlation between successive observations, and the presence of this auto-correlation can generate spurious results during statistical inference (Murphy et al., 2010). Such observations are not 'independent and identically distributed' (i.i.d.), leading to misinterpretation of the strength of evidence obtained in statistical analyses (Hargrove and Pickering, 1992). When performing inference between two or more time series, lagged cross-correlation interacts with each pattern of auto-correlation, causing errors due to temporal pseudoreplication (i.e., observations in time which lack independent replication) that are not

Table 2
Sixty-one-day analysis period with average (range) of daily fluxes and key environmental conditions for each site during that period. NEE: net ecosystem exchange of carbon; E: evapotranspiration; H: sensible heat flux; D: vapour pressure deficit; θ: soil water content; R_n: net radiation; BR: Bowen ratio (= Σ[H] / Σ[L_v E]; L_v E: latent heat flux).

Site	Date range/Season	NEE (g m^{-2} d^{-1})	E (mm d^{-1})	H (MJ m^{-2} d^{-1})	D (kPa)	θ (m^3 m^{-3})	T_a (°C)	R_n (MJ m^{-2} d^{-1})	BR (-)
AU-TTE [a]	15/1–17/3/2017	−1.7	3.1	4.7	2.40	0.047	28.4	15.2	0.7
	Summer–Autumn	(−2.0–0.4)	(1.2–4.8)	(0.5–7.3)	(0.93–3.51)	(0.018–0.14)	(22.1–32.1)	(2.1–21.7)	(0.2–1.4)
AU-ASM [a]	15/1–17/3/2011	−0.2	2.8	5.5	1.75	0.092	27.3	15.0	1.3
	Summer–Autumn	(−1.7–2.3)	(0.7–5.1)	(0.9–13.2)	(0.25–4.46)	(0.034–0.26)	(22.8–34.9)	(5.3–19.9)	(0.2–6.5)
AU-Stp	15/2–17/4/2011	−1.9	4.0	2.4	0.98	0.22	25.9	11.9	0.2
	Summer–Autumn	(−4.4–−0.1)	(1.5–6.0)	(0.0–4.0)	(0.36–1.82)	(0.11–0.27)	(21.4–28.5)	(2.5–18.5)	(0.0–0.6)
AU-Otw	1/9–31/10/2009	−1.7	1.4	0.2	0.26	0.36	11.1	4.0	1.2
	Spring	(−3.8–2.0)	(0.4–3.3)	(−3.0–2.1)	(0.00–0.7)	(0.22–0.42)	(7.7–21.2)	(0.2–7.5)	(0.2–3.2)
AU-DaP	31/12/2012–2/3/2013	−3.8	4.5	0.7	0.98	0.13	27.8	13.1	0.0
	Wet	(−7.3–0.4)	(1.0–6.2)	(−1.5–3.9)	(0.34–1.65)	(0.061–0.18)	(24.0–31.1)	(1.4–17.8)	(−0.2–0.4)
NZ-Oxf	15/12/2006–14/2/2007	−0.1	1.9	2.0	0.43	0.50	13.5	8.4	1.1
	Summer	(−5.7–4.6)	(0.03–7.7)	(−2.6–5.8)	(0.06–1.57)	(0.46–0.52)	(7.3–21.7)	(−0.4–18.0)	(−17.2–7.5)
AU-Rig	5/6–5/8/2014	−2.3	1.0	−0.3	0.20	0.49	8.6	2.4	0.0
	Winter	(−3.9–0.5)	(0.5–3.1)	(−3.0–2.0)	(0.00–0.51)	(0.38–0.52)	(4.2–13.3)	(−0.8–5.8)	(−1.0–0.7)
AU-Gat	17/8–17/10/2015	−3.2	1.2	1.0	0.51	0.20	11.8	7.1	0.6
	Winter–Spring	(−7.1–2.0)	(0.1–4.0)	(−3.3–6.2)	(0.09–2.38)	(0.10–0.28)	(5.9–23.2)	(1.4–13.0)	(−1.9–3.6)
AU-Emr	5/2–6/4/2012	0.3	1.8	5.0	1.37	0.13	25.3	12.7	1.7
	Summer–Autumn	(−4.4–3.2)	(0.4–4.3)	(0.3–8.1)	(0.22–2.12)	(0.08–0.21)	(21.6–29.3)	(2.9–18.3)	(0.1–6.0)
AU-Sam	15/12/2011–14/2/2012	−2.2	2.4	2.8	0.82	0.51	23.1	12.1	0.5
	Summer	(−4.9–2.4)	(1.1–4.3)	(0.3–5.5)	(0.24–2.41)	(0.39–0.58)	(18.8–28.0)	(3.8–20.1)	(0.1–1.0)
NZ-BFu [b]	19/1–21/3/2014	−2.1	2.3	2.7	0.38	0.15	13.8	9.4	0.5
	Summer–Autumn	(−6.8–4.0)	(0.2–5.3)	(−4.8–8.2)	(0.01–1.60)	(0.11–0.21)	(7.8–20.7)	(−0.4–17.7)	(−1.7–1.8)
NZ-ADn [c]	22/1–24/3/2018	−1.0	2.4	1.8	0.50	0.22	16.3	10.1	0.3
	Summer–Autumn	(−8.5–4.6)	(−0.1–6.5)	(−8.5–7.5)	(0.05–1.52)	(0.10–0.35)	(9.2–24.0)	(1.4–19.2)	(−4.8–1.5)
AU-Lox	11/11/2008–11/1/2009	−6.3	6.5	−1.8	1.35	0.11	20.0	17.3	−0.1
	Spring–Summer	(−9.0–2.2)	(2.8–9.7)	(−10.6–2.8)	(0.36–2.92)	(0.08–0.15)	(11.8–27.4)	(5.3–22.2)	(−0.6–0.2)
AU-Cm1 [d]	4/12/2010–3/2/2011	−15.4	5.6	−0.3	1.48	not measured	23.2	18.6	−0.02
(Maize)	Summer	(−22.9–−1.2)	(2.6–8.0)	(−6.9–3.9)	(0.46–3.45)		(13.9–32.1)	(3.9–23.7)	(−0.4–0.3)
AU-Cm1 [d]	8/8–8/10/2011	−4.9	2.4	0.3	0.76	not measured	16.0	7.1	0.07
(Wheat)	Winter–Spring	(−8.8–0.9)	(0.9–5.1)	(−4.0–3.4)	(0.08–3.02)		(7.4–26.5)	(−0.8–12.2)	(−0.9–0.7)
AU-Cm2 [d]	15/12/2010–14/2/2011	−9.7	5.9	−1.9	1.10	not measured	22.0	21.5	−0.1
	Summer	(−14.7–−1.8)	(3.3–9.5)	(−6.7–1.9)	(0.12–2.64)		(13.4–29.1)	(6.1–27.7)	(−0.4–0.2)
NZ-Sco	15/12/2008–14/2/2009	−2.8	3.7	2.5	0.64	0.42	17.6	14.8	0.3
	Summer	(−7.0–7.3)	(1.1–5.9)	(−0.5–6.2)	(0.25–1.07)	(0.28–0.57)	(14.1–23.3)	(4.1–20.7)	(−0.1–1.3)
NZ-BFm [b]	15/12/2013–14/2/2014	−2.9	3.4	0.5	0.38	0.35	13.9	11.7	0.2
	Summer	(−9.7–3.4)	(0.2–8.0)	(−6.2–5.4)	(0.00–1.54)	(0.22–0.51)	(10.0–20.5)	(1.2–18.7)	(−0.7–1.8)
NZ-ADw [c]	22/1–24/3/2018	−0.7	2.8	0.6	0.45	0.22	16.5	10.1	−1.5
	Summer–Autumn	(−6.4–5.2)	(0.0–8.3)	(−8.9–7.0)	(0.06–1.17)	(0.16–0.27)	(10.2–22.8)	(1.4–19.1)	(−107–2.9)

[a,b,c,d] paired sites indicated with the same letter

affected by measurement frequency or persistence of environmental conditions. Thus, time series violate several fundamental assumptions in statistics and probability theory (e.g., temporal pseudoreplication, auto-correlation, lagged cross-correlation; Hargrove and Pickering, 1992; Murphy et al., 2010). By contrast, the characteristics of wavelet analysis (linearity, localisation in time, energy conservation) make wavelets ideal for statistical inference of time series by interpreting variance in the time series instead of the observations themselves (He and Guan, 2013; He et al., 2014b). This approach invokes the Central Limit Theorem by assuming that auto-correlation in variances is negligible relative to auto-correlation in the observations. Wavelets are finite, cyclic functions that are modulated to identify fluctuations in time and timescale through dilation and translation of a *mother wavelet* (Ψ). Thus, wavelets are ideal for analysis of data with intermittencies or nonstationarities, such as fluxes (Stoy et al., 2005, 2013; van Gorsel et al., 2013).

A multivariate version of wavelet multiple linear regression (wMLR) was used to infer the relative importance of driving variables on the turbulent fluxes (NEE, E and H). Seven variables were considered as potential drivers of the three fluxes (R_n, T_a, θ, D, q, T_s and G). The complete analysis was performed in three steps: 1) wavelet coherence was used to determine the timescale of peak correlation (a_{max}) between fluxes and environmental factors, where a_{max} was used in the following two analyses; 2) wavelet principal components analysis (wPCA; Cleverly et al., 2016a) was performed independently for each site to identify dependencies (i.e., coupling) amongst (i) NEE, E and H (fluxPCs) or (ii) environmental factors (envPCs); and 3) wPCA was combined with wMLR to infer relationships between environmental factors and fluxes (i.e., wavelet canonical correlation analysis, wCCA) at a timescale of a_{max}.

First (step 1), a_{max} was identified using wavelet coherence analysis to estimate the correlation between fluxes and environmental factors (Grinsted et al., 2004; Shi et al., 2014; Torrence and Compo, 1998). Fluxes and environmental factors were represented by their main principal components (fluxPCs, envPCs), as described in step (2), except PCs in this step were determined using details at all scales which were supported by the length of a given time series. Coherence between two variables represents the squared-correlation, r^2, and wavelet coherence analysis uses a continuous wavelet transformation (CWT) to estimate r^2. The Morlet wavelet was chosen as Ψ for its functional similarity to turbulence (Cuxart et al., 2002) and its improved compositing (Schaller et al., 2017). Analysis of timescales was limited to 10 scales per octave. Significant coherence was determined using Monte Carlo methods and a red noise auto-regressive null model. Two primary modes of variability were identified, at daily and annual timescales, despite minor differences in coherence across management intensities (Fig. S2). Thus, analyses were performed at a daily timescale.

Next (step 2), dependencies amongst environmental factors were identified using wPCA (Matlab R2013a, The MathWorks Inc., Natick Massachusetts USA). In wPCA, the covariance matrix is populated from the product of paired wavelet coefficients. wPCA is limited to the discrete wavelet transformation (DWT) to simplify construction of the

covariance matrix and for computational efficiency. Normalised data were used to account for differences in units amongst environmental factors (equivalent to the use of a correlation matrix as a basis for computation of eigenvalues λ_i and associated eigenvectors). Time series were padded to the next octave j (where the sample size is 2^j) with spectrally neutral values (i.e., the first or last value in the time series) to minimise errors due to the cone of influence. A second-order symlet was chosen for Ψ due to its improved localisation in the frequency domain relative to a first-order 'Haar' wavelet and improved symmetry over the second-order Daubechies wavelet upon which it is based. The resultant linear combinations of environmental factors (X_p) are defined as:

$$envPC_i = \alpha_{i,1}X_1 + \cdots + \alpha_{i,p}X_p \quad (1)$$

where envPC$_i$ is the ith principal component, α_i is the component loading for envPC$_i$ and p is the number of environmental factors. Similarly, wPCs of the fluxes (fluxPC$_i$) were determined as fluxPC$_i$ = $\alpha_{i,NEE}$ NEE + $\alpha_{i,E}$ E + $\alpha_{i,H}$ H. Principal components are defined to be orthogonal, meaning they are independent for the purposes of multiple regression analysis (i.e., no colinearity). Principal components with cumulative eigenvalues ($\lambda_1 + \cdots + \lambda_i$) explaining 70% or more of the total variability ($\Sigma\lambda_p$) were included in following analyses. fluxPC$_1$ was retained in favour of the original fluxes when its eigenvalue exceeded 70% of the total variability in the fluxes. Variables with a component loading of less than 10% of the total loadings were considered to be independent (i.e., not colinear). wPCA included details for scales 2^1–2^x (number of 30-min periods) and approximations at a scale of 2^x, with x representing the highest integer scale below a_{max}.

Time series of the principal components were constructed from wPCA-derived loadings α_1–α_p (e.g., Eq. (1)) and normalised environmental factors or fluxes. A CWT was performed on wPCs to provide samples for wCCA. The Mexican hat wavelet is defined as the second derivative of a Gaussian function (Collineau and Brunet, 1993), and it is effective at locating nonstationarities precisely in time (Schaller et al., 2017). Thus, coefficients from the Mexican hat wavelet represent directional variance by integrating information on timing (Percival and Walden, 2000), validating the application of the Central Limit Theorem and establishing that statistics based upon coefficients from the Mexican hat wavelet represent direct functional responses in one variable to perturbations in another. However, CWT is oversampled, erroneously inflating sample size and degrees of freedom (Katul and Parlange, 1995). Thus, daily-scale variance was computed as the sum of each day's wavelet coefficients. For the Central Limit Theorem to apply, a sample size of at least 30 is required, thus restricting our ability to form rigorous inferences of inter-annual fluxes for sites with a data record which is shorter than 30 years, and this is why daily fluctuations were evaluated in this study.

Initially, the primary mode of variability in the fluxes (fluxPC$_1$) was regressed against (i) the k number of envPCs which explained a cumulative 70% of the variability in those variables (envPC$_1$–envPC$_k$) and (ii) any other environmental factors which contributed less than 10% of the variability to any of envPC$_1$–envPC$_k$ (X_a … X_n); for example:

$$fluxPC_i \sim \beta_{i,0} + \beta_{i,1}X_a + \cdots + \beta_{i,n}X_n + \beta_{i,n+1}envPC_1 + \cdots + \beta_{i,n+k}envPC_k + \beta_{i,n+k+1}X_a \times \cdots \times X_n + \varepsilon \quad (2)$$

where each β is a unique regression coefficient, the term with coefficient β_{n+k+1} is the interaction for X_n non-colinear environmental factors when $n > 1$, and ε is the regression error term.

Next, envPCs which were not significantly related to fluxPC$_1$ were removed and replaced by any variables which contributed to less than 10% of the variability in the remaining envPCs. In cases where multiple variables were at risk of introducing colinearity in subsequent regression models, each variable which was introduced by removal of an envPC$_i$ was evaluated individually. This is illustrated in the following example, where (i) envPC$_2$ of two envPCs was not significantly related to fluxPC$_1$, (ii) all X_1–X_p contributed more than 10% to the combination of envPC$_1$ and envPC$_2$, and (iii) three of X_1–X_p contribute more than 10% of the variability in envPC$_2$ but not in envPC$_1$ (X_x, X_y, X_z):

$$fluxPC_i \sim \beta_{i,0} + \beta_{i,1}X_x + \beta_2 envPC_1 + \varepsilon \quad (3a)$$

$$fluxPC_i \sim \beta_{i,0} + \beta_{i,1}X_y + \beta_2 envPC_1 + \varepsilon \text{and} \quad (3b)$$

$$fluxPC_i \sim \beta_{i,0} + \beta_{i,1}X_z + \beta_2 envPC_1 + \varepsilon \quad (3c)$$

The complete stepwise procedure was repeated for (i) fluxPC$_2$ or (ii) any of NEE, E or H which represented less than 10% of the loadings on fluxPC$_1$, wherever either was applicable. The linear importance of each environmental factor for predicting fluxes was estimated from the product of that factor's α in envPC$_i$ and the regression coefficient (β) for that envPC$_i$, but only if β were significantly different from zero. The importance of each environmental factor for the prediction of fluxes was estimated as $\Sigma|\beta_{i,X}|$ or $\Sigma|\alpha_{i,X}\,\beta_{i,envPCi}|$ for significant main effects and envPCs, respectively.

All analyses were performed in Matlab R2018b (The Mathworks, Inc., Natick, Massachusetts, USA), and inferences were based upon a sample size of $N = 61$ days. The probability of a type I error was presumed to be 0.05 ($p < 0.05$) in all hypothesis tests. Because of the nature of wavelet transformation, the equivalent of a multivariate analysis of variance could not be performed. We thus acknowledge that lacking a single statistical model for all 19 sites increases the probability of an erroneous inference for a site. The coefficient of determination (R^2) for wMLR and wCCA will be distinguished as a capital letter in this study to avoid confusion with coherence or squared correlation, r^2. Negative statistical coefficients for NEE were taken to indicate increasing values of NEP (NEP = −NEE).

All statistical outputs (including those of intermediate steps) and data used in this study can be obtained from the TERN OzFlux data portal (Cleverly, 2019). Example Matlab instructions for data analyses can be found in the Supplementary Material S2.

6. Results

6.1. Management intensity and coupling amongst fluxes

Five combinations of dependencies amongst NEE, E and H were identified across the 19 sites, based upon the sign of their component loadings in wPCA (Table 3). Examples of Type 1 dependencies amongst fluxes were found in every management intensity class, although Type 1 dominated in the highly intense management class (Fig. 2, Table S1). Increases in NEP were synchronised with increasing E and H (Type 1) at

Table 3
Coupling amongst fluxes from wavelet Principal Components Analysis (wPCA). fluxPC$_1$: principal component explaining the largest proportion of total variability amongst the fluxes; α: Component loading for NEE (α_1), E (α_2) and H (α_3), respectively. fluxPC1 term not shown for component loadings < 10% of total loadings.

Type	fluxPC$_1$	Productivity–E coupling	Productivity–H coupling	E–H coupling	Explanation
Type 1	{$-\alpha_1$ NEE, $+\alpha_2$ E, $+\alpha_3$ H}	coupled	coupled	coupled	full physiological coupling, no heat stress
Type 2	{$-\alpha_1$ NEE, $-\alpha_3$ H}	uncoupled	reverse	uncoupled	heat stress, evaporative cooling
Type 3	{$-\alpha_1$ NEE, $+\alpha_2$ E, $-\alpha_3$ H}	coupled	reverse	reverse	heat stress, isohydric
Type 4	{$-\alpha_1$ NEE, $-\alpha_2$ E}	reverse	uncoupled	uncoupled	low D, no heat stress
Type 5	{$-\alpha_1$ NEE, $-\alpha_2$ E, $+\alpha_3$ H}	reverse	coupled	reverse	low D, energy limited

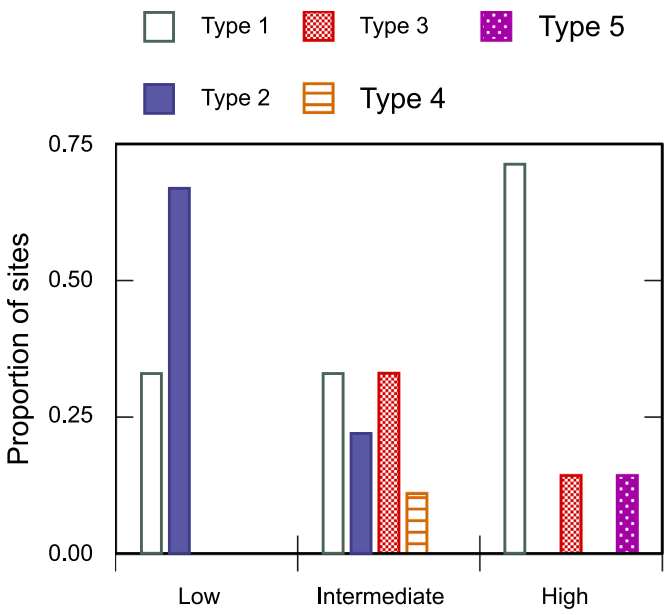

Fig. 2. The relative proportion of sites showing each of the wavelet PCA component loading types for fluxes in each management class (low, intermediate, high). Refer to Table 3 for a description of flux coupling types.

nine locations (Table S1).

Only Type 1 and Type 2 dependencies were observed in the grazed rangelands of this study. In Type 2 and Type 3 dependencies, decreasing NEE (i.e., increasing NEP) was synchronised with decreasing H, indicative of a negative heat stress response. For Type 2, variation in E represented less than 10% of the total flux variability and was thus considered to be uncoupled from fluctuations in NEE or H. Type 2 relationships were observed at four rangeland and pasture sites (Fig. 2, Table S1). Type 3 relationships in which NEP was positively correlated to E and inversely correlated to H occurred on four of the 19 farms (Table S1). Positive coupling with E on the highly managed Ashley Dene Farm (NZ-ADw) was small in magnitude, comparable to that of Type 2 dependencies on farms with intermediate-intensity management (Table S1). Reverse coupling between NEP and E was uncommon, observed at only one site for each of Type 4 and Type 5 dependencies. Refer to Table S1 for individual results from each of the 19 sites.

6.2. Coupling amongst environmental factors

Complete wPCA results for the seven environmental factors are also provided in Table S1. Interactions amongst environmental factors were generally site specific, varying across sites in the identity and strength of contributing variables and in the amount of variation explained by envPCs (Fig. S3). Thus, dependencies amongst environmental factors were evaluated in detail at the paired sites to minimise differences introduced by the large distances between farms in this study (Fig. 3).

In grazed rangelands, R_n and G maintained similar relationships across Pine Hill Station (AU-ASM, AU-TTE), whereas T_a, T_s, θ and q showed a *ca.* 180° phase shift relative to the R_n–G axis across sites (Fig. 3a, d). In the comparison of an irrigated and fertilised pasture (NZ-BFu) versus a kale forage crop (NZ-BFm), fluctuations of T_s and θ differed across the two datasets; irrigation and fertilisation induced a shift from coupling of T_s with R_n to coupling of T_s with T_a, and highly intense management induced a shift in coupling for θ from D to q, representing a release of θ from atmospheric water stress (Fig. 3b, e). In lucerne, fluctuations in G and q differed between irrigated and unirrigated paddocks on Ashley Dene farm, whereas relative coupling amongst R_n, D, T_a and T_s were fixed (NZ-ADn, NZ-ADw; Fig. 3c, f). In irrigated broadacre crops of the Coleambally Irrigation Area, fluctuations in T_s and q were similarly correlated in winter (AU-Cm1 wheat) and summer (AU-Cm1 maize, AU-Cm2 rice; Fig. 3g–i). With the exception of D, heavy irrigation for the cultivation of rice created similar relationships amongst environmental factors as irrigated cultivation of wheat during the winter and spring, but T_a dominance in winter (Fig. 3g) was exchanged for R_n dominance in summertime irrigated rice (Fig. 3i). Across all comparisons, some environmental factors maintained the same contribution to total environmental variability at paired sites, whereas other environmental factors were rotated relative to the fixed factors, suggesting that management can influence some environmental factors, but others are beyond management control.

6.3. Management responses of fluxes to environmental factors

R^2 from wCCA for the regression of fluctuations in NEE, E and H against fluctuations in meteorological and edaphic conditions ranged from 0.16 at AU-Emr to 0.88 at AU-Gat (Fig. 4). Values of R^2 in Fig. 4 for NEE, E or H which were not different at a given site were obtained from a single wCCA model, and only values of R^2 which were significantly different from zero are presented in Fig. 4. Representing predictability of variations in fluxes, R^2 did not show consistent patterns across management intensity classes, but there were some general trends. Grazed rangelands had small R^2 as a group (0.34 ± 0.06), with a range of values (0.17–0.54) which overlapped completely with the range of R^2 values from sites managed at intermediate intensity (0.16–0.88, 0.55 ± 0.07). By contrast, the range of R^2 for grazed rangelands overlapped only slightly with the range of R^2 from highly intense management (0.42–0.84, 0.62 ± 0.07). Similar to the grazed rangelands, the range of R^2 values for sites with high-intensity management overlapped completely with the range of R^2 values from intermediate-intensity management (Fig. 4). No relationships between R^2 and ϕ were apparent in grazed rangelands (Fig. 4). At sites with intermediate-intensity management, the smallest values of R^2 were observed at intermediate ϕ (R^2 = 0.28–0.35; NZ-ADn, AU-DaP, AU-Otw), with the exception of low R^2 for rainfed crops at AU-Emr (R^2 = 0.16). Amongst sites with highly intense management, R^2 was highest in the three irrigated farms with the highest ϕ (R^2 = 0.78–0.84; AU-Lox almonds, AU-Cm1 maize, NZ-Sco dairy; Fig. 4).

In all except three cases, a single inference model was obtained, with only envPCs and factors which were not co-linear with the envPCs explaining fluctuations in NEE, E and H (Table S2, Fig. S3). This indicates that fluxes generally responded to coupled environmental factors instead of individually to those environmental factors. One exception was in irrigated maize (AU-Cm1), where fluctuations in q were co-linear with $envPC_2$ and not $envPC_1$, but fluctuations in q alone (amongst the co-linear factors in $envPC_2$) were significantly related to variation in NEE, E and H ($\beta_q = -0.06 \pm 0.01$, $p < 0.001$) without contributions from other co-linear factors in $envPC_2$ ($\beta_{envPC2} = -0.06 \pm 0.06$, $p = 0.35$) ($R^2 = 0.79$, $p < 0.001$; Fig. 5). This site provides an example of a strong environment–flux relationship due to both individual factors (q) and interacting environmental factors (R_n and D; cf. Fig. 5, Table S1).

The improved pasture AU-Otw similarly showed fluctuations in D to contribute to explaining fluctuations in NEE, E and H from outside of $envPC_2$, although strong nonlinearities were present which reduced the strength of statistical inference for all environmental factors at this site (R^2 = 0.11–0.28, p = < 0.001–0.03; Table S2, Fig. 6). In this example, the full model with $envPC_1$ and $envPC_2$, along with non-colinear R_n, resulted in no values of β_X which were significantly different from zero (β_{Rn}, β_{envPC1} and β_{envPC2} of −0.009 ± 0.04, −0.15 ± 0.11 and 0.03 ± 0.11, respectively; Table S2) and a small R^2 which was nonetheless significantly different from zero ($R^2 = 0.11$, $p = 0.02$). This discrepancy was likely induced by nonlinearity in the residuals, particularly near values of zero on the x-axis which represent a large range of fluctuations in NEE, E and H under stable environmental conditions (Fig. 6). D contributed little to $envPC_1$ at this site, so removal

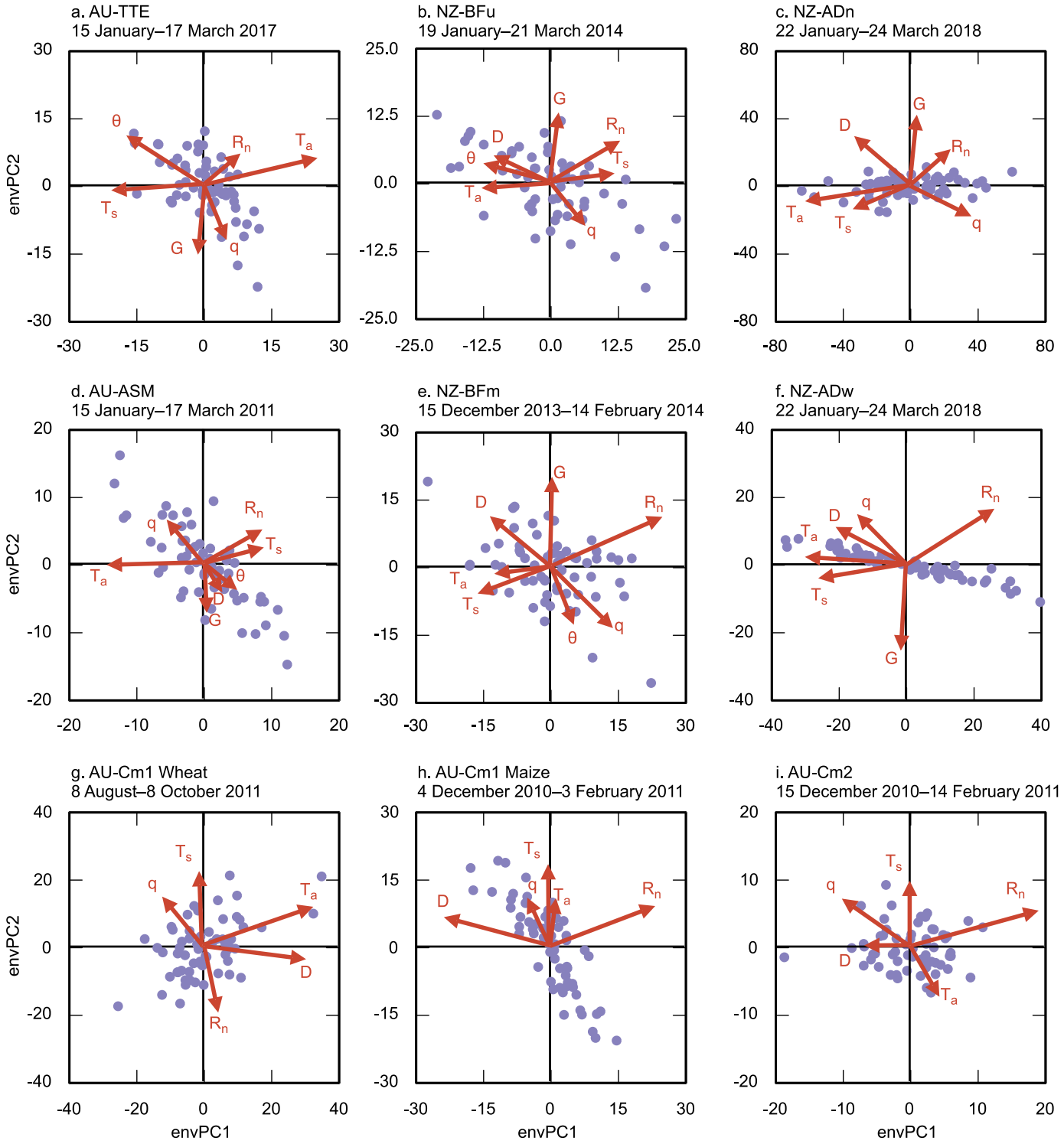

Fig. 3. Wavelet PCA at the paired sites. Paired sites were grazed rangeland (a, d; AU-ASM, AU-TTE), irrigated/fertilised dairy pasture (b; NZ-BFm) versus unirrigated/unfertilised forage crop kale (e; NZ-BFu), irrigated/fertilised versus unirrigated/unfertilised forage crop lucerne (c, f; NZ-ADw, NZ-ADn), and irrigated broadacre crops (g, h, i; AU-Cm1 wheat, maize, AU-Cm2 rice).

of $envPC_2$ from the regression permitted the inclusion of D as a main effect. Doing so resolved the discrepancy between model and submodel results, showing a weak linearity in fluxes with respect to fluctuations in D without losing nonlinear effects near the y-axis (Fig. 6).

Strong nonlinearities were observed at many sites (Fig. S3), with an example from grazed rangeland AU-ASM shown in Fig. 7. For $fluxPC_1$, the response was largely linear (R^2 = 0.54), but with notable nonlinearities in the residuals. This suggests that environment–flux relationships contain a linear portion and a nonlinear portion, the latter due to lags in the cycles of perturbation and response (Fig. 7). Nonlinear responses were dominant for E (R^2 = 0.34; Fig. 7), suggesting that the sensitivity of E to precipitation pulses is largely independent of climate conditions in central Australia.

No single environmental factor accounted for fluctuations in NEE, E and H, and there was much variability across sites within each management intensity class (Fig. 8). The most important factors for

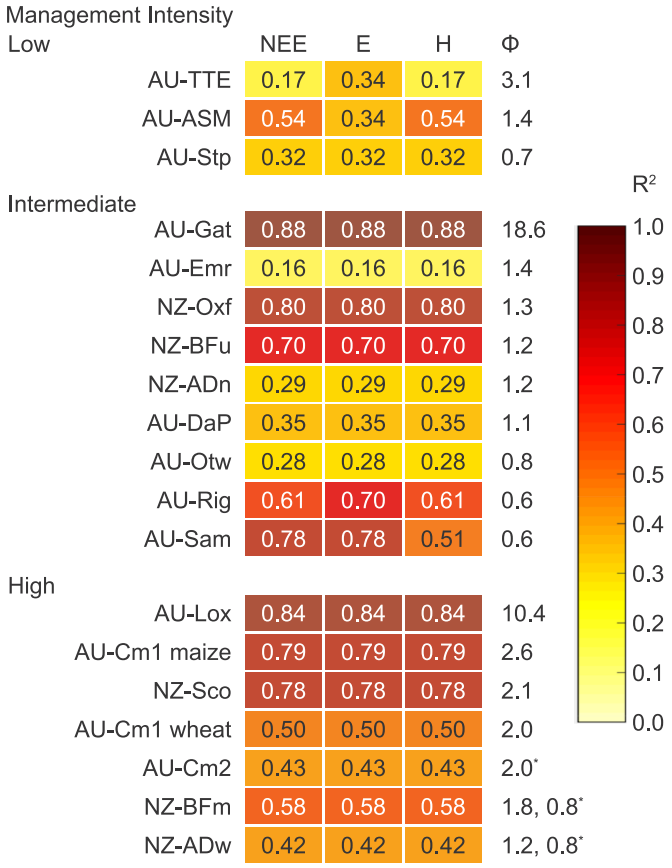

Fig. 4. Heat map of coefficients of determination (R^2) from wCCA. Sites are arranged within a management-intensity class according to their short-term aridity index (ϕ). Values of ϕ marked by an asterisk included farm-scale irrigation amounts.

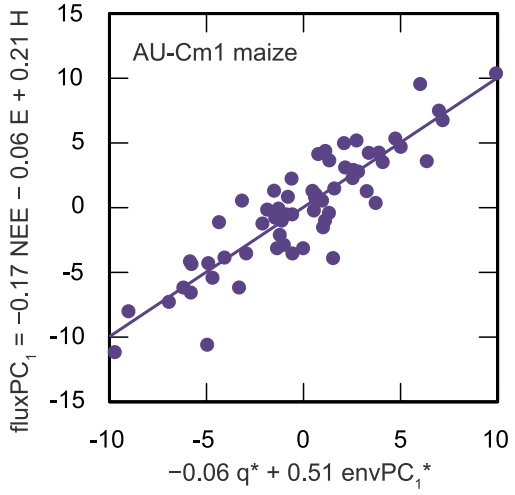

Fig. 5. wCCA results for an example irrigated broadacre crop. See supplementary material for details of regression statistics (Table S2, Fig. S1). Asterisks represent factors with coefficients significantly different from zero.

explaining linear responses of fluxes in grazed rangelands (importance > 15%) were T_s, T_a and G (0.23 ± 0.11, 0.19 ± 0.09 and 0.17 ± 0.11, respectively; Fig. 8). In intermediate-intensity management, most environmental factors were important for predicting fluxes: T_a, R_n, G and D (0.15 ± 0.02, 0.12 ± 0.03, 0.25 ± 0.08 and 0.17 ± 0.06, respectively; Fig. 8). Environmental factor importance was similar to intermediate-management in highly intense

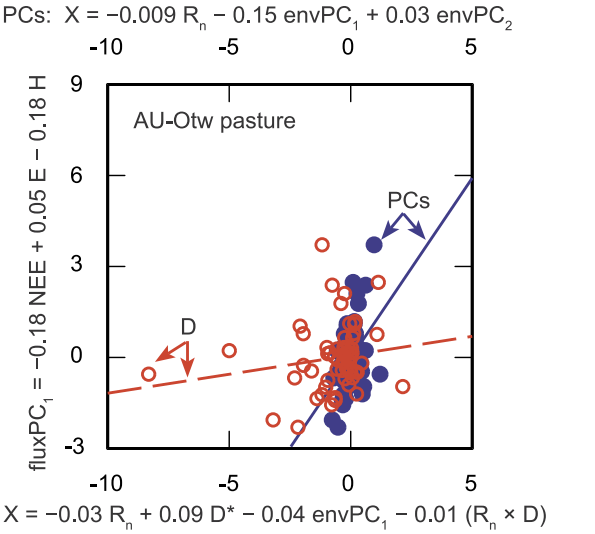

Fig. 6. wCCA results for an example improved pasture. See supplementary material for details of regression statistics (Table S2, Fig. S1). 'PCs' statistical model: closed symbols, solid line and top abscissa axis; 'D' model: open circles, dashed line and bottom abscissa. Asterisks represent factors with coefficients significantly different from zero.

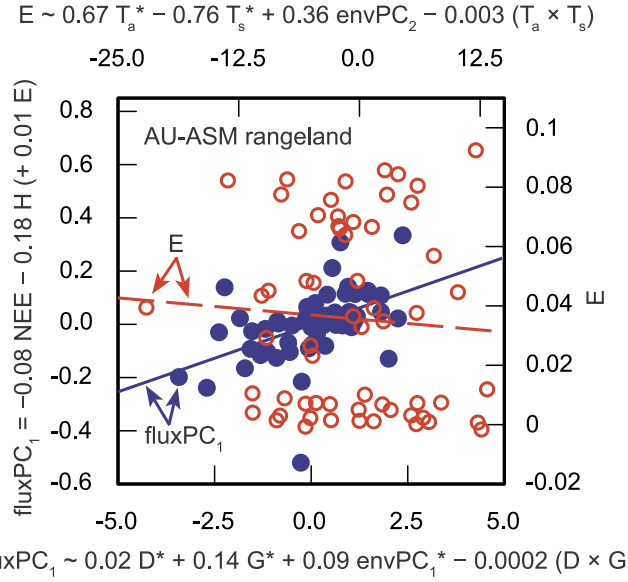

Fig. 7. wCCA results for an example and grazed rangeland. See supplementary material for details of regression statistics (Table S2, Fig. S1). fluxPC1: closed circles, solid line, bottom abscissa and left ordinate axes; 'E': open circles, dashed line, top abscissa and right ordinate. Asterisks represent factors with coefficients significantly different from zero.

management, except that T_a was replaced by θ: θ, R_n, G and D (0.16 ± 0.05, 0.20 ± 0.04, 0.16 ± 0.03 and 0.27 ± 0.11, respectively; Fig. 8).

7. Discussion

Simple regression of environmental factors alone has been previously found to fit measured fluxes better than the output of land-surface models, although the reasons for this have not yet been identified (Best et al., 2015; Haughton et al., 2018b). Nonetheless, no consensus has been reached regarding identification of the key environmental factors driving variations in surface fluxes, which is still an active area of inquiry. Thus, a call has been issued for more studies to

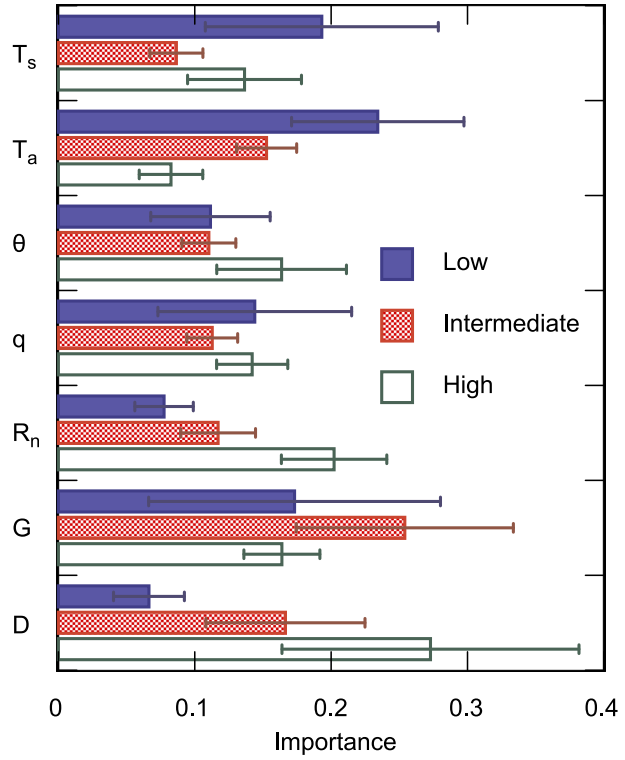

Fig. 8. Proportional importance (± standard error) of environmental factors in wCCA for each management intensity class (low, intermediate, high).

evaluate climate and management effects using paired and multiple towers (Mudge et al., 2011). In this study, we used a multivariate wavelet–statistics conjunction approach to evaluate management effects on relationships between fluctuations in environmental factors and synchronised fluctuations of carbon, water and heat fluxes (NEE, E and H, respectively). Coupling amongst fluxes showed some key differences across management intensity categories, providing partial but not overwhelming support for hypothesis 1. By contrast, coupling amongst environmental factors appeared to be strongly site-specific and showed inconsistent effects of management in comparison of paired sites at a single location, thus failing to support our hypothesis that increasingly intense management would weaken integration of environmental factors (hypothesis 2). Despite site-specific coupling amongst environmental factors, we found relationships between fluxes and environmental factors to depend upon management intensity and the short-term level of aridity within a management intensity class (Fig. 4), providing support for hypothesis 3. However, no single environmental factor was found which explained variability in fluctuations of NEE, E or H, consistent with previous findings (Hao et al., 2018); for example, enhanced vegetation index, photosynthetically active radiation and air temperature were all found to be significantly correlated to E by Wagle et al. (2017b). Instead, the way in which environmental factors co-varied through time (i.e., their synchronised interaction) affected variations in NEE, E and H, especially in water-limited landscapes where precipitation pulses dominate the coordination of fluxes and environmental factors (Cleverly et al., 2013).

7.1. Coupling of carbon, water and energy cycles

The largest effect of management identified in this study was upon the relationship amongst fluxes. Even though examples of full, positive coupling between NEP, E and H (Type 1, {−NEE, +E, +H}) were found for each management intensity class in our study (on nine farms), the proportion of sites showing such full coupling increased with increasingly intense management (Fig. 2). Intense management practices like irrigation and fertilisation are intended to minimise the impact of detrimental environmental conditions and maximise yield, thus generating synchronisation amongst carbon, water and energy fluxes. There can be regional variation in the response of crops to heat and water stress (Dreccer et al., 2018), although managing for heat stress can be as simple as converting from dryland agriculture or pasture to irrigated agriculture, if enough water is available. Because many irrigated broadacre cropping and arboreal horticultural systems exist in water-limited climates with high evaporative demand and the potential for plant stress (Stokes et al., 2008; Williams et al., 2002), as they do in the Australian examples of this study, they can require substantial volumes of irrigation water to return a profitable yield. Irrigated almonds in this study (AU-Lox) did not show any apparent stress, with coupling of NEP, E and H. Irrigation can protect against physiological stress and stress-induced crop failure by ameliorating heat extremes through evaporative cooling (Chen et al., 2017; Cleverly et al., 2016b, 2015; Stevens et al., 2012), in addition to supporting high productivity at high T_a or D and lengthening the growing season over which NEE is below zero (Mueller et al., 2017; Wagle et al., 2017a).

Decoupling between NEP and E has been proposed for vegetation experiencing heat stress, when photosynthetic assimilation declines whilst transpiration is maintained for cooling of the leaf (De Kauwe et al., 2019). Reverse coupling between H and NEP implies a negative response to heat, as has been observed during heatwaves (van Gorsel et al., 2016; van Heerwaarden and Teuling, 2014). We found that reverse coupling between H and NEP (i.e., NEP was increasing when H was declining) occurred at another eight sites in the current study, with locations where E was decoupled from NEP and H (Type 2) tending to be more common in hot, minimally managed environments, and where NEP and E were both reverse coupled to H (Type 3) on colder, more highly managed farms (Fig. 2). The first and primary role of management in Australia and New Zealand was thus identified as supporting positive coupling amongst NEP, E and H and thereby managing crop stress, whether that stress originated from lack of water or abundance of heat.

7.2. Season, energy limitation and aridity

Year-round growing conditions across much of Australia and New Zealand favour a strong wintertime net carbon sink (i.e., NEE < 0), when low temperature limits respiration and heat stress (Campbell et al., 2014; Cleverly et al., 2013; Hutley et al., 2005; Renchon et al., 2018). For example, heavy irrigation was required in the summer for rice to obtain similar relationships amongst environmental factors as were seen in irrigated wheat during winter and spring months (Fig. 3g, i). However, wintertime cropping comes at a cost of supporting about half of the productivity as that of summer cropping, thus only three out of 19 locations in this study were evaluated during winter. Furthermore, productivity of winter pasture can be reverse-coupled to turbulent heating (e.g., AU-Otw), suggesting that some grasslands in Australia can be susceptible to heat stress, even during winter. Seasonal differences in evaporative fraction (LE / R_n) exist between irrigated wheat and maize (0.83 and 0.57, respectively; Lei and Yang, 2010), reflecting smaller potential energy limitations during wintertime than during summer. Similarly, we found that environmental factors responded most strongly to fluctuations in R_n for maize (and rice), but that they responded to fluctuations in T_a for wheat (i.e., they had the largest α coefficient value in $envPC_1$).

The response of vegetation to changes in environmental factors critically depends upon whether productivity and E in a given ecosystem are energy or water limited (Donohue et al., 2009; Restrepo-Coupe et al., 2016). In energy-limited ecosystems, water is plentiful, but cloud cover restricts R_n (Hutley et al., 2005; Kanniah et al., 2013; Whitley et al., 2011). R_n and D both drive variations of E in energy-limited regions (Zhang et al., 2017), where they are strongly coherent (Peng et al., 2018). Consistent with previous observations, R_n and D

were strongly and negatively coherent in this study for energy-limited regions and in areas where irrigation released water limitations, except for winter wheat, in which T_a was strongly coherent with D instead due to seasonal limitations on R_n (Fig. 3). In water-limited environments, the relationship of θ and q shifted from the woody rangeland (AU-ASM) to the grass-dominated rangeland (AU-TTE). θ is typically only related to E in water-limited environments when θ is above the wilting point (Akuraju et al., 2017), explaining the variable levels of θ coupling at AU-ASM and AU-TTE. Vegetation at AU-ASM is suspected to have an effect on surface θ via hydraulic redistribution (Cleverly et al., 2016b), thus reducing the dependence of fluxes on θ and providing an alternative explanation for the lack of correlation with θ near the surface at AU-ASM. Regardless of variations in the importance of individual environmental factors, interactions amongst all environmental factors were generally strong across our study, as has been previously inferred at AU-ASM using boundary analysis (Cleverly et al., 2013; Eamus et al., 2016).

The 19 sites in this study showed a large range of energy versus water limitations as indicated by ϕ, in which energy limitation was defined by values below unity (i.e., R_n / [ρ_w L_v] > P) and degree of water limitation by values above unity (i.e., R_n / [ρ_w L_v] > P; Fig. 4). The Canterbury Plains in New Zealand (NZ-Oxf, NZ-ADn, NZ-ADw, NZ-BFu, NZ-BFm) are generally energy limited, although a lack of precipitation during the late summer commonly pushes ϕ above unity (Graham et al., 2016), and this was when large NEP was identified for analysis in the current study (Table 2). Values of ϕ near unity are likely to reflect co-limitations by energy and water (Cleverly et al., 2013; Ryu et al., 2008). Currently, a general shift from energy limitations to water limitations appears to be occurring in the climate system (Babst et al., 2019), making an understanding of crop responses to this transition critical. By increasing θ, irrigation can tip a crop back to an energy-limited state, although irrigation ultimately depends upon heavy precipitation to replenish water supplies in Australia's drylands, providing only opportunistic access to irrigation in regions where irrigated agricultural production might not be sustainable over the long term (Garnaut, 2008; Khan and Hanjra, 2009; Vote et al., 2015).

7.3. Predictability, phenology and nonlinearities

Controls on fluxes in warmer, drier climates such as those of tropical Australia can be site specific, making fluxes more unpredictable and difficult to represent without local parameterisation in land surface models (Haughton et al., 2018a). As a consequence, we found that predictability as inferred from R^2 was low on the five northern farms in our study (AU-DaP, AU-Stp, AU-ASM, AU-TTE, AU-Emr; $R^2 < 0.55$, cf. Figs. 1 and 4). Nonlinearities in regressions for these sites are consistent with the presence of time-lagged perturbations to fluxes after environmental conditions have returned to normal (i.e., as with pulse-response dynamics), thus acting to desynchronise environmental conditions and ecosystem responses (Huxman et al., 2004). In the woody central Australian rangeland site (AU-ASM), E responded exclusively to precipitation pulses, with equal sensitivity to large and small fluctuations in environmental factors (Fig. 7). This variability in sensitivity to climate during precipitation pulses of varying intensity thus forms the basis for variable responses of water-use efficiency (WUE = NEP / E) observed at this location (Eamus et al., 2013; Tarin et al., 2020). Pulse behaviour during the summer of 2010/2011 was produced by heavy precipitation (Boening et al., 2012; Fasullo et al., 2013; Poulter et al., 2014) in widespread, organised weather patterns which imposed cycles of strong energy limitations (Cleverly et al., 2013, 2016a). Thus, similarities in the responses of irrigated rice and grazed rangeland were associated with similar weather patterns during the growing season at AU-ASM and AU-Cm2, despite contrasting water requirements for the rice crop at AU-Cm2 and for forage plants AU-ASM. Wavelet transformation of environmental factors and fluxes can provide the first quantitative framework for evaluating sensitivity to precipitation pulses, for which further study is merited.

Outside of the five northern sites (AU-DaP, AU-Stp, AU-ASM, AU-TTE, AU-Emr), R^2 followed two patterns relative to aridity, depending upon management intensity. For intermediate-intensity management, R^2 was small at locations where water and energy limitations were balanced ($0.8 \leq \phi \leq 1.2$; NZ-ADn, AU-Otw; $R^2 = 0.28$–0.29, cf. Figs. 1 and 4). This suggests that water limitations and energy limitations can counteract one another over time, resulting in no observed net effect of environmental factors on fluxes. This situation can potentially create a conundrum for land surface models, where a small imbalance between compensating environmental factors can bias the output (Haughton et al., 2018b). Intra-seasonal shifts in phenology, for example due to grazing or harvesting, can also degrade the predictability of NEE, E and H from environmental factors. Examples of phenological control of fluxes, instead of environmental control, were found at NZ-ADw, NZ-ADn and NZ-BFm, all of which were exposed to 2–3 defoliation events during the analysis period. During regrowth, NEE and E were constrained by low leaf area index instead of energy or water limitations. To account for phenological effects, one could integrate data regarding vegetation structure (e.g., leaf area index, vegetation indices), but these data would need to be measured at an equivalent frequency to that of fluxes and environmental factors. Altogether for intermediate-intensity management, we found three factors that reduced the innate predictability of fluxes: (i) nonlinear effects of precipitation pulses; (ii) complementarity amongst coupled environmental factors in their effects on fluxes, as when water and energy limitations are in temporal balance within a single season; and (iii) by undocumented shifts in phenology.

In contrast to patterns of predictability for intermediate-intensity management, those for highly intense management fell into two categories depending upon aridity: irrigation in more water-limiting conditions ($\phi > 2$, AU-Lox almonds, AU-Cm1 maize and NZ-Sco dairy pasture) resulted in high flux predictability ($R^2 > 0.75$, Fig. 4), whereas moderate flux predictability ($R^2 = 0.62 \pm 0.07$) was found for sites with low values of ϕ ($\phi \leq 2$, AU-Cm1 wheat, AU-Cm2 rice, and NZ-BFm dairy farm and NZ-ADw irrigated lucerne). Even though there are environmental factors beyond the control of irrigation, irrigation practices are finely attuned to affect the environmental factors which are related to productivity, water use and heat flux, and these effects are magnified in regions where there is a large difference between on-farm and adjacent natural conditions. The most extreme example is from irrigated almonds during the final year of the Millennium Drought, where intense sensible heat advection onto the irrigated orchard from surrounding semi-arid lands pushed H to as low as -500 W m^{-2} (i.e., an input of energy into the orchard; Stevens et al., 2012). Termed "the oasis effect," horizontal transport of energy across steep environmental gradients created by differential irrigation and evaporative cooling results in coherent variation in fluxes and scalars across the landscape (Brakke et al., 1978; Brunet et al., 1994; Cooper et al., 2003; Hanks et al., 1971). As a consequence, irrigation in Australia can lead to very high daily values of NEP in crops, both in this study (NEE *ca.* -23 g m^{-2} d^{-1} at a minimum for AU-Cm1 maize) and in previous research on rice, maize and sugarcane, which reached productivity rates of NEE = -40 μmol m^{-2} s^{-1} during the peak of the summer growing season (Vote et al., 2015; Webb et al., 2018).

This survey of environmental drivers for fluctuations in NEE, E and H leaves open a number of limitations and uncertainties which merit further investigation. These can be characterised as (i) incomplete information on carbon budgets; (ii) lack of information for relating productivity and water use to yield; and (iii) the inherent challenge of resolving reasonable relationships from nonlinear systems undergoing high levels of variability. For (i), one missing component in this study is an accounting of net biome production (NBP), which can show very different contributions to the total carbon budget from NEE. For example, a crop might be assessed as a carbon sink from NEE alone, whereas accounting for export of carbon via harvest as NBP can shift

the carbon budget to a net source (Buysse et al., 2017). Even in the absence of such a shift from carbon sink to source, failing to account for export of dissolved organic carbon from crops can result in a very large overestimation of carbon sink strength by NEE relative to NBP (Kindler et al., 2011; Webb et al., 2018). Second (ii), there are strong relationships between biomass and yield in Australian agriculture (Donohue et al., 2018), implying a close relationship between NEE (or NBP) and yield. Peak-season carbon fluxes are the most predictive for annual carbon budgets (Zscheischler et al., 2016), thus the results of our study would be particularly informative for parameterising agricultural yield models like APSIM (e.g., Donohue et al., 2018; He et al., 2014a; Luo et al., 2018; Ummenhofer et al., 2015). Third (iii), variability in precipitation is an important yet often overlooked constraint on vegetative productivity in pastures and rangelands, and this variability also affects grazing strategies in Australia (Sloat et al., 2018). Ecohydrological processes are often strongly nonlinear, amplifying intermittency and unpredictability when precipitation variability is high (Porporato et al., 2015). We found evidence for the presence of three types of nonlinearity: (a) organisation of fluxes and environmental factors around intermittent precipitation pulses; (b) over-riding control of crop phenology by mowing or grazing; and (c) compensatory effects of one or more environmental factors which ameliorated the effects of other factors. These types of nonlinearities are due to abrupt changes in biotic or environmental conditions, which are not captured well by land-surface models or analytical methods that require stationarity (e.g., auto-regression; De Keersmaecker et al., 2015). We present for the first time an analytical framework for quantifying pulse–response sensitivities on a single scale by using a wavelet–statistics conjunction approach which can incorporate information on the timing of fluctuations in addition to simple lagged averages, a necessity for land surface modelling which has recently been elucidated by Haughton et al. (2018b).

8. Conclusions

In this survey of agricultural ecosystems across Australia and New Zealand, we developed a novel statistical framework through wavelet–statistics conjunction to incorporate information on temporal synchronisation between variations in turbulent fluxes (NEE, E and H) and environmental factors (R_n, q, T_a, T_s, D, G and θ). Using this approach to test hypotheses about the effects of management on environment–flux relationships, we found that:

1 Coordination amongst NEE, E and H was strongly affected by management practices as hypothesised. Full coupling of NEE, E and H was more frequently achieved through irrigation and fertilisation practices than in minimally grazed rangelands and pastures. Decoupling of NEP and E was observed at drier sites, some of which also showed reverse coupling to H, illustrating the decoupling of carbon and water fluxes in response to conditions conducive of heat stress (De Kauwe et al., 2019).
2 We could not fully support our second hypothesis that coordination amongst environmental factors would be related to management. Large-scale differences in relationships amongst environmental factors were observed across the 19 sites of this study, suggesting that environmental conditions are largely site-specific and outside of management control. Comparison of paired sites across management intensity categories, seasons and crop types identified some environmental factors which had fixed effects across paired sites, whereas dependencies with other environmental factors differed amongst sites. This suggests that a subset of environmental factors are under management control at a given location, whereas other environmental factors represent constraints on the agricultural system.
3 The combination of management practices which promote positive coupling of carbon and water budgets (i.e., point 1) with site-specific variability of coupling amongst environmental factors (i.e., point 2) generated various patterns in the predictability of fluxes from environmental factors. Predictability was small in northern Australian agriculture as hypothesised by Haughton et al. (2018a), with low R^2 due to nonlinear responses of fluxes and environmental factors, including those due to precipitation pulses in hot climate zones. Predictability (as a function of R^2) was also low for farms where (i) complementarity between energy and water limitations was apparent ($0.8 \leq \phi \leq 1.2$) and (ii) management activities such as grazing or harvesting induced a phenological response and release from environmental constraints. Conversely, irrigation in water-limited environments resulted in very high predictability of variations in fluxes from knowledge of environmental factors.

By incorporating timing and temporal variability into a statistical framework, wavelet–regression conjunction modelling has the capability of transforming our understanding of how ecosystems respond to fluctuations in climate, to the occurrence of nonstationarities such as precipitation pulses and extreme weather events, and to climate change by helping to analytically separate the effects of fluctuations, nonstationarities and trends. Several potential applications arise from this work, including analysis of longer-term phenological trends characterised by satellite imagery, development of a better understanding of drought impacts on crops, comparison of crops with differing physiognomy, and analysis of greenup/brown-down dynamics.

Declaration of Competing Interest

The authors declare that they have no known competing financial interests or personal relationships that could have appeared to influence the work reported in this paper.

Acknowledgements

The study used data from Terrestrial Ecosystem Research Network (TERN, http://tern.org.au), supported by the Australian Government through the National Collaborative Research Infrastructure Strategy (NCRIS). The authors would like to further acknowledge funding through the Australian Research Council (ARC) and the National Water Commission through Programs3 (surface water–groundwater interactions, AU-TTE) and 4 (groundwater–vegetation–atmosphere interactions, AU-Gat) of the National Centre for Groundwater Research and Training (a part of the NCRIS Groundwater project). Further funding for AU-Gat was provided by ARC and the Victoria Department of Economic Development, Jobs, Transport and Resources (ARC LP140100871). NZ funding sources included Landcare Researchand NZ government. We would also like to thank Eva van Gorsel for her insights and discussion during early planning stages of this study, and two anonymous reviewers whose suggestions have helped to improve manuscript quality.

Supplementary materials

Supplementary material associated with this article can be found, in the online version, at doi:10.1016/j.agrformet.2020.107934.

References

Abry, P., Didier, G., 2018. Wavelet eigenvalue regression for n-variate operator fractional Brownian motion. J. Multivar. Anal. 168, 75–104. https://doi.org/10.1016/j.jmva.2018.06.007.

Adamson, D., Loch, A., Schwabe, K., 2017. Adaptation responses to increasing drought frequency. Aust. J. Agr. Resour. Econ. 61, 385–403. https://doi.org/10.1111/1467-8489.12214.

Akuraju, V.R., Ryu, D., George, B., Ryu, Y., Dassanayake, K., 2017. Seasonal and interannual variability of soil moisture stress function in dryland wheat field, Australia. Agric. For. Meteor. 232, 489–499. https://doi.org/10.1016/j.agrformet.2016.10.007.

Australian Bureau of Statistics, 2018. Agricultural Commodities. Commonwealth of Australia, AustraliaCanberra, pp. 2016–2017.

Babst, F., Bouriaud, O., Poulter, B., Trouet, V., Girardin, M.P., Frank, D.C., 2019. Twentieth century redistribution in climatic drivers of global tree growth. Sci. Adv. 5https://doi.org/10.1126/sciadv.aat4313. eaat4313.

Behtari, B., Jafarian, Z., Alikhani, H., 2019. Temperature sensitivity of soil organic matter decomposition in response to land management in semi-arid rangelands of Iran. Catena 179, 210–219. https://doi.org/10.1016/j.catena.2019.03.043.

Beringer, J., Hutley, L.B., Abramson, D., Arndt, S.K., Briggs, P., Bristow, M., Canadell, J.G., Cernusak, L.A., Eamus, D., Edwards, A.C., Evans, B.J., Fest, B., Goergen, K., Grover, S.P., Hacker, J., Haverd, V., Kanniah, K., Livesley, S.J., Lynch, A., Maier, S., Moore, C., Raupach, M., Russell-Smith, J., Scheiter, S., Tapper, N.J., Uotila, P., 2015. Fire in Australian savannas: from leaf to landscape. Glob. Change Biol. 21, 62–81. https://doi.org/10.1111/gcb.12686.

Beringer, J., Hutley, L.B., Hacker, J.M., Neininger, B., U, K.T.P., 2011. Patterns and processes of carbon, water and energy cycles across northern Australian landscapes: from point to region. Agric. For. Meteor. 151, 1409–1416. https://doi.org/10.1016/j.agrformet.2011.05.003.

Beringer, J., Hutley, L.B., McHugh, I., Arndt, S.K., Campbell, D., Cleugh, H.A., Cleverly, J., Resco de Dios, V., Eamus, D., Evans, B., Ewenz, C., Grace, P., Griebel, A., Haverd, V., Hinko-Najera, N., Huete, A., Isaac, P., Kanniah, K., Leuning, R., Liddell, M.J., Macfarlane, C., Meyer, W., Moore, C., Pendall, E., Phillips, A., Phillips, R.L., Prober, S.M., Restrepo-Coupe, N., Rutledge, S., Schroder, I., Silberstein, R., Southall, P., Yee, M.S., Tapper, N.J., van Gorsel, E., Vote, C., Walker, J., Wardlaw, T., 2016. An introduction to the Australian and New Zealand flux tower network – OzFlux. Biogeosciences 13, 5895–5916. https://doi.org/10.5194/bg-13-5895-2016.

Beringer, J., McHugh, I., Hutley, L.B., Isaac, P., Kljun, N., 2017. Technical note: dynamic INtegrated gap-filling and partitioning for OzFlux (DINGO). Biogeosciences 14, 1457–1460. https://doi.org/10.5194/bg-14-1457-2017.

Berko, H., Etheridge, D., Loh, D., Kuske, T., Colin, A., Gregory, R., Spencer, D., Law, R., Zegelin, S., Feitz, A., 2012. Installation Report for Arcturus (ARA): an inland Baseline Station For the Continuous Measurement of Atmospheric Greenhouse gases. 1922103616. Geoscience Australia, Canberra.

Best, M.J., Abramowitz, G., Johnson, H.R., Pitman, A.J., Balsamo, G., Boone, A., Cuntz, M., Decharme, B., Dirmeyer, P.A., Dong, J., Ek, M., Guo, Z., Haverd, V., Van den Hurk, B.J.J., Nearing, G.S., Pak, B., Peters-Lidard, C., Santanello Jr., J.A., Stevens, L., Vuichard, N., 2015. The plumbing of land surface models: benchmarking model performance. J. Hydrometeor. 16, 1425–1442. https://doi.org/10.1175/JHM-D-14-0158.1.

Boening, C., Willis, J.K., Landerer, F.W., Nerem, R.S., Fasullo, J., 2012. The 2011 La Niña: so strong, the oceans fell. Geophys. Res. Lett. 39, L19602. https://doi.org/10.1029/2012gl053055.

Brakke, T.W., Verma, S.B., Rosenberg, N.J., 1978. Local and regional components of sensible heat advection. J. Appl. Meteor. 17, 935–963.

Brown, M., Whitehead, D., Hunt, J.E., Clough, T.J., Arnold, G.C., Baisden, W.T., Sherlock, R.R., 2009. Regulation of soil surface respiration in a grazed pasture in New Zealand. Agric. For. Meteor. 149, 205–213. https://doi.org/10.1016/j.agrformet.2008.08.005.

Brunet, Y., Itier, B., McAneney, J., Lagouarde, J.P., 1994. Downwind evolution of scalar fluxes and surface resistance under conditions of local advection. Part II: Measurements over barley. Agric. For. Meteor. 71, 227–245.

Budyko, M.I., 1974. Climate and Life. Academic Press, San Diego, CA 508 pp.

Buysse, P., Bodson, B., Debacq, A., De Ligne, A., Heinesch, B., Manise, T., Moureaux, C., Aubinet, M., 2017. Carbon budget measurement over 12 years at a crop production site in the silty-loam region in Belgium. Agric. For. Meteor. 246, 241–255. https://doi.org/10.1016/j.agrformet.2017.07.004.

Cai, Q., Zhang, Y.L., Sun, Z.X., Zheng, J.M., Bai, W., Zhang, Y., Liu, Y., Feng, L.S., Feng, C., Zhang, Z., Yang, N., Evers, J.B., Zhang, L.Z., 2017. Morphological plasticity of root growth under mild water stress increases water use efficiency without reducing yield in maize. Biogeosciences 14, 3851–3858.

Cammarano, D., Tian, D., 2018. The effects of projected climate and climate extremes on a winter and summer crop in the southeast USA. Agric. For. Meteor. 248, 109–118. https://doi.org/10.1016/j.agrformet.2017.09.007.

Campbell, D.I., Smith, J., Goodrich, J.P., Wall, A.M., Schipper, L.A., 2014. Year-round growing conditions explains large CO_2 sink strength in a New Zealand raised peat bog. Agric. For. Meteor. 192, 59–68. https://doi.org/10.1016/j.agrformet.2014.03.003.

Chen, X., Su, Z., Ma, Y., Cleverly, J., Liddell, M., 2017. An accurate estimate of monthly mean land surface temperatures from MODIS clearsky retrievals. J. Hydrometeor. 18, 2827–2847. https://doi.org/10.1175/jhm-d-17-0009.1.

Chi, J., Waldo, S., Pressley, S., O'Keeffe, P., Huggins, D., Stöckle, C., Pan, W.L., Brooks, E., Lamb, B., 2016. Assessing carbon and water dynamics of no-till and conventional tillage cropping systems in the inland Pacific Northwest US using the eddy covariance method. Agric. For. Meteor. 218-219, 37–49. https://doi.org/10.1016/j.agrformet.2015.11.019.

Cleverly, J., 2019. Agricultural ecosystems collection. TERN OzFlux: Australian and New Zealand Flux Research and Monitoring Network, http://hdl.handle.net/102.100.100/79013.

Cleverly, J., Boulain, N., Villalobos-Vega, R., Grant, N., Faux, R., Wood, C., Cook, P.G., Yu, Q., Leigh, A., Eamus, D., 2013. Dynamics of component carbon fluxes in a semi-arid *Acacia* Woodland, Central Australia. J. Geophys. Res.: Biogeosci. 118, 1168–1185. https://doi.org/10.1002/jgrg.20101.

Cleverly, J., Eamus, D., Edwards, W., Grant, M., Grundy, M.J., Held, A., Karan, M., Lowe, A.J., Prober, S.M., Sparrow, B., Morris, B., 2019. TERN, Australia's land observatory: addressing the global challenge of forecasting ecosystem responses to climate variability and change. Environ. Res. Lett. 14, 095004. https://doi.org/10.1088/1748-9326/ab33cb.

Cleverly, J., Eamus, D., Luo, Q., Restrepo Coupe, N., Kljun, N., Ma, X., Ewenz, C., Li, L., Yu, Q., Huete, A., 2016a. The importance of interacting climate modes on Australia's contribution to global carbon cycle extremes. Sci. Rep. 6, 23113. https://doi.org/10.1038/srep23113.

Cleverly, J., Eamus, D., Restrepo Coupe, N., Chen, C., Maes, W., Li, L., Faux, R., Santini, N.S., Rumman, R., Yu, Q., Huete, A., 2016b. Soil moisture controls on phenology and productivity in a semi-arid critical zone. Sci. Total Environ. 568, 1227–1237. https://doi.org/10.1016/j.scitotenv.2016.05.142.

Cleverly, J., Eamus, D., Van Gorsel, E., Chen, C., Rumman, R., Luo, Q., Restrepo Coupe, N., Li, L., Kljun, N., Faux, R., Yu, Q., Huete, A., 2016c. Productivity and evapotranspiration of two contrasting semiarid ecosystems following the 2011 global carbon land sink anomaly. Agric. For. Meteor. 220, 151–159. https://doi.org/10.1016/j.agrformet.2016.01.086.

Cleverly, J., Thibault, J.R., Teet, S.B., Tashjian, P., Hipps, L.E., Dahm, C.N., Eamus, D., 2015. Flooding regime impacts on radiation, evapotranspiration and latent heat fluxes over groundwater-dependent riparian cottonwood and saltcedar forests. Adv. Meteorol. 2015, 935060. https://doi.org/10.1155/2015/935060.

Collineau, S., Brunet, Y., 1993. Detection of turbulent coherent motions in a forest canopy part I: wavelet analysis. Bound.-Lay. Meteor. 65, 357–379. https://doi.org/10.1007/bf00707033.

Cooper, D., Eichinger, W., Archuleta, J., Hipps, L., Kao, J., Leclerc, M., Neale, C., Prueger, J., 2003. Spatial source-area analysis of three-dimensional moisture fields from LIDAR, eddy covariance, and a footprint model. Agric. For. Meteor. 114, 213–234.

Cunningham, S.C., Mac Nally, R., Baker, P.J., Cavagnaro, T.R., Beringer, J., Thomson, J.R., Thompson, R.M., 2015. Balancing the environmental benefits of reforestation in agricultural regions. Perspect. Plant Ecol. Evol. Syst. 17, 301–317. https://doi.org/10.1016/j.ppees.2015.06.001.

Cuxart, J., Morales, G., Terradellas, E., Yague, C., 2002. Study of coherent structures and estimation of the pressure transport terms for the nocturnal stable boundary layer. Bound.-Lay. Meteor. 105, 305–328. https://doi.org/10.1023/a:1019974021434.

Davis, P.A., Brown, J.C., Saunders, M., Lanigan, G., Wright, E., Fortune, T., Burke, J., Connolly, J., Jones, M.B., Osborne, B., 2010. Assessing the effects of agricultural management practices on carbon fluxes: spatial variation and the need for replicated estimates of Net Ecosystem Exchange. Agric. For. Meteor.

De Kauwe, M.G., Medlyn, B.E., Pitman, A.J., Drake, J.E., Ukkola, A., Griebel, A., Pendall, E., Prober, S., Roderick, M., 2019. Examining the evidence for decoupling between photosynthesis and transpiration during heat extremes. Biogeosciences 16, 903–916. https://doi.org/10.5194/bg-16-903-2019.

De Keersmaecker, W., Lhermitte, S., Tits, L., Honnay, O., Somers, B., Coppin, P., 2015. A model quantifying global vegetation resistance and resilience to short-term climate anomalies and their relationship with vegetation cover. Glob. Ecol. Biogeogr. 24, 539–548. https://doi.org/10.1111/geb.12279.

Donohue, R.J., Lawes, R.A., Mata, G., Gobbett, D., Ouzman, J., 2018. Towards a national, remote-sensing-based model for predicting field-scale crop yield. Field Crop. Res. 227, 79–90. https://doi.org/10.1016/j.fcr.2018.08.005.

Donohue, R.J., McVicar, T.R., Roderick, M.L., 2009. Climate-related trends in Australian vegetation cover as inferred from satellite observations, 1981-2006. Glob. Change Biol. 15, 1025–1039.

Dreccer, M.F., Fainges, J., Whish, J., Ogbonnaya, F.C., Sadras, V.O., 2018. Comparison of sensitive stages of wheat, barley, canola, chickpea and field pea to temperature and water stress across Australia. Agric. For. Meteor. 248, 275–294.

Dresel, P.E., Dean, J.F., Perveen, F., Webb, J.A., Hekmeijer, P., Adelana, S.M., Daly, E., 2018. Effect of Eucalyptus plantations, geology, and precipitation variability on water resources in upland intermittent catchments. J. Hydrol. 564, 723–739. https://doi.org/10.1016/j.jhydrol.2018.07.019.

Drewniak, B.A., Mishra, U., Song, J., Prell, J., Kotamarthi, V.R., 2015. Modeling the impact of agricultural land use and management on US carbon budgets. Biogeosciences 12, 2119–2129.

Eamus, D., Cleverly, J., Boulain, N., Grant, N., Faux, R., Villalobos-Vega, R., 2013. Carbon and water fluxes in an arid-zone *Acacia* savanna woodland: an analyses of seasonal patterns and responses to rainfall events. Agric. For. Meteor. 182–183, 225–238. https://doi.org/10.1016/j.agrformet.2013.04.020.

Eamus, D., Huete, A., Cleverly, J., Nolan, R.H., Ma, X., Tarin, T., Santini, N.S., 2016. Mulga, a major tropical dry open forest of Australia: recent insights to carbon and water fluxes. Environ. Res. Lett. 11, 125011. https://doi.org/10.1088/1748-9326/11/12/125011.

Ellis, N.R., Albrecht, G.A., 2017. Climate change threats to family farmers' sense of place and mental wellbeing: a case study from the Western Australian Wheatbelt. Soc. Sci. Med. 175, 161–168. https://doi.org/10.1016/j.socscimed.2017.01.009.

Etheridge, D., Luhar, A., Loh, Z., Leuning, R., Spencer, D., Steele, P., Zegelin, S., Allison, C., Krummel, P., Leist, M., van der Schoot, M., 2011. Atmospheric monitoring of the CO2CRC Otway project and lessons for large scale CO_2 storage projects. Energy Procedia 4, 3666–3675. https://doi.org/10.1016/j.egypro.2011.02.298.

Fasullo, J.T., Boening, C., Landerer, F.W., Nerem, R.S., 2013. Australia's unique influence on global sea level in 2010-2011. Geophys. Res. Lett. 40, 4368–4373. https://doi.org/10.1002/grl.50834.

Foley, J.A., DeFries, R., Asner, G.P., Barford, C., Bonan, G., Carpenter, S.R., Chapin, F.S., Coe, M.T., Daily, G.C., Gibbs, H.K., Helkowski, J.H., Holloway, T., Howard, E.A., Kucharik, C.J., Monfreda, C., Patz, J.A., Prentice, I.C., Ramankutty, N., Snyder, P.K., 2005. Global consequences of land use. Science 309, 570–574. https://doi.org/10.1126/science.1111772.

Garnaut, R., 2008. The Garnaut climate Change Review : Final Report / Ross Garnaut. Cambridge University Press, Port Melbourne, Vic.

Graham, S.L., Kochendorfer, J., McMillan, A.M.S., Duncan, M.J., Srinivasan, M.S., Hertzog, G., 2016. Effects of agricultural management on measurements, prediction, and partitioning of evapotranspiration in irrigated grasslands. Agric. Water Manage. 177, 340–347. https://doi.org/10.1016/j.agwat.2016.08.015.

Grinsted, A., Moore, J.C., Jevrejeva, S., 2004. Application of the cross wavelet transform

and wavelet coherence to geophysical time series. Nonlinear Process Geophys 11, 561–566.
Guan, H., He, X., Zhang, X., 2015. A comprehensive examination of global atmospheric CO_2 teleconnections using wavelet-based multi-resolution analysis. Environ. Earth Sci. 74, 7239–7253. https://doi.org/10.1007/s12665-015-4705-z.
Hanks, R.J., Allen Jr., L.H., Gardner, H.B., 1971. Advection and evapotranspiration of wide-row sorghum in the Central Great Plains. Agron. J. 63, 520–527.
Hao, X.M., Zhang, S.H., Li, W.H., Duan, W.L., Fang, G.H., Zhang, Y., Guo, B., 2018. The uncertainty of Penman-Monteith method and the energy balance closure problem. J. Geophys. Res.: Atmos. 123, 7433–7443. https://doi.org/10.1029/2018jd028371.
Hargrove, W.W., Pickering, J., 1992. Pseudoreplication: a *sine qua non* for regional ecology. Landsc. Ecol 6, 251–258. https://doi.org/10.1007/bf00129703.
Haughton, N., Abramowitz, G., De Kauwe, M.G., Pitman, A.J., 2018a. Does predictability of fluxes vary between FLUXNET sites? Biogeosciences 15, 4495–4513. https://doi.org/10.5194/bg-15-4495-2018.
Haughton, N., Abramowitz, G., Pitman, A.J., 2018b. On the predictability of land surface fluxes from meteorological variables. Geosci. Model Dev. 11, 195–212. https://doi.org/10.5194/gmd-11-195-2018.
He, L., Cleverly, J., Chen, C., Yang, X., Li, J., Liu, W., Yu, Q., 2014a. Diverse responses of winter wheat yield and water use to climate change and variability on the semiarid Loess Plateau in China. Agron. J. 106, 1169–1178. https://doi.org/10.2134/agronj13.0321.
He, L., Cleverly, J., Wang, B., Jin, N., Mi, C., Liu, D.L., Yu, Q., 2018. Multi-model ensemble projections of future extreme heat stress on rice across southern China. Theor. Appl. Climatol. 133, 1107–1118. https://doi.org/10.1007/s00704-017-2240-4.
He, X., Guan, H., 2013. Multiresolution analysis of precipitation teleconnections with large-scale climate signals: a case study in South Australia. Water Resour. Res. 49, 6995–7008. https://doi.org/10.1002/wrcr.20560.
He, X., Guan, H., Zhang, X., Simmons, C.T., 2014b. A wavelet-based multiple linear regression model for forecasting monthly rainfall. Int. J. Climatol. 34, 1898–1912. https://doi.org/10.1002/joc.3809.
Hsu, K., Gupta, H.V., Gao, X., Sorooshian, S., Imam, B., 2002. Self-organizing linear output map (SOLO): an artificial neural network suitable for hydrologic modeling and analysis. Water Resour. Res. 38, 1302. https://doi.org/10.1029/2001wr000795.
Hunt, J.E., Laubach, J., Barthel, M., Fraser, A., Phillips, R.L., 2016. Carbon budgets for an irrigated intensively grazed dairy pasture and an unirrigated winter-grazed pasture. Biogeosciences 13, 2927–2944. https://doi.org/10.5194/bg-13-2927-2016.
Hutley, L.B., Beringer, J., Isaac, P.R., Hacker, J.M., Cernusak, L.A., 2011. A sub-continental scale living laboratory: spatial patterns of savanna vegetation over a rainfall gradient in northern Australia. Agric. For. Meteor. 151, 1417–1428. https://doi.org/10.1016/j.agrformet.2011.03.002.
Hutley, L.B., Leuning, R., Beringer, J., Cleugh, H.A., 2005. The utility of the eddy covariance techniques as a tool in carbon accounting: tropical savanna as a case study. Aust. J. Bot. 53, 663–675. https://doi.org/10.1071/BT04147.
Huxman, T.E., Snyder, K.A., Tissue, D., Leffler, A.J., Ogle, K., Pockman, W.T., Sandquist, D.R., Potts, D.L., Schwinning, S., 2004. Precipitation pulses and carbon fluxes in semiarid and arid ecosystems. Oecologia 141, 254–268. https://doi.org/10.1007/s00442-004-1682-4.
Isaac, P., Cleverly, J., McHugh, I., van Gorsel, E., Ewenz, C., Beringer, J., 2017. OzFlux data: network integration from collection to curation. Biogeosciences 14, 2903–2928. https://doi.org/10.5194/bg-14-2903-2017.
Jeong, S.-J., Ho, C.-H., Piao, S., Kim, J., Ciais, P., Lee, Y.-B., Jhun, J.-G., Park, S.K., 2014. Effects of double cropping on summer climate of the North China Plain and neighbouring regions. Nat. Clim. Change. 4, 615. https://doi.org/10.1038/nclimate2266.
Jin, Z., Zhuang, Q.L., Wang, J.L., Archontoulis, S.V., Zobel, Z., Kotamarthi, V.R., 2017. The combined and separate impacts of climate extremes on the current and future US rainfed maize and soybean production under elevated CO_2. Glob. Change Biol. 23, 2687–2704. https://doi.org/10.1111/gcb.13617.
Kanniah, K.D., Beringer, J., Hutley, L., 2013. Exploring the link between clouds, radiation, and canopy productivity of tropical savannas. Agric. For. Meteor. 182–183, 304–313. https://doi.org/10.1016/j.agrformet.2013.06.010.
Katul, G.G., Parlange, M.B., 1995. The spatial structure of turbulence at production wavenumbers using orthonormal wavelets. Bound.-Lay. Meteor. 75, 81–108. https://doi.org/10.1007/bf00721045.
Khan, S., Hanjra, M.A., 2009. Footprints of water and energy inputs in food production - Global perspectives. Food Policy 34, 130–140.
Kindler, R., Siemens, J., Kaiser, K., Walmsley, D.C., Bernhofer, C., Buchmann, N., Cellier, P., Eugster, W., Gleixner, G., Grunwald, T., Heim, A., Ibrom, A., Jones, S.K., Jones, M., Klumpp, K., Kutsch, W., Larsen, K.S., Lehuger, S., Loubet, B., McKenzie, R., Moors, E., Osborne, B., Pilegaard, K., Rebmann, C., Saunders, M., Schmidt, M.W.I., Schrumpf, M., Seyfferth, J., Skiba, U., Soussana, J.F., Sutton, M.A., Tefs, C., Vowinckel, B., Zeeman, M.J., Kaupenjohann, M., 2011. Dissolved carbon leaching from soil is a crucial component of the net ecosystem carbon balance. Glob. Change Biol. 17, 1167–1185. https://doi.org/10.1111/j.1365-2486.2010.02282.x.
Kirschbaum, M.U.F., Schipper, L.A., Mudge, P.L., Rutledge, S., Puche, N.J.B., Campbell, D.I., 2017. The trade-offs between milk production and soil organic carbon storage in dairy systems under different management and environmental factors. Sci. Total Environ. 577, 61–72. https://doi.org/10.1016/j.scitotenv.2016.10.055.
Lara, M.J., Johnson, D.R., Andresen, C., Hollister, R.D., Tweedie, C.E., 2017. Peak season carbon exchange shifts from a sink to a source following 50 + years of herbivore exclusion in an Arctic tundra ecosystem. J. Ecol. 105, 122–131. https://doi.org/10.1111/1365-2745.12654.
Laubach, J., Hunt, J.E., 2018. Greenhouse-gas budgets for irrigated dairy pasture and a winter-forage kale crop. Agric. For. Meteor. 258, 117–134. https://doi.org/10.1016/j.agrformet.2017.04.013.
Laubach, J., Hunt, J.E., Graham, S.L., Buxton, R.P., Rogers, G.N.D., Mudge, P.L., Carrick, S., Whitehead, D., 2019. Irrigation increases forage production of newly established lucerne but enhances net ecosystem carbon losses. Sci. Total Environ. 689, 921–936. https://doi.org/10.1016/j.scitotenv.2019.06.407.
Lei, H., Yang, D., 2010. Interannual and seasonal variability in evapotranspiration and energy partitioning over an irrigated cropland in the North China Plain. Agric. For. Meteor. 150, 581–589.
Loh, Z., Leuning, R., Zegelin, S., Etheridge, D., Bai, M., Naylor, T., Griffith, D., 2009. Testing Lagrangian atmospheric dispersion modelling to monitor CO_2 and CH_4 leakage from geosequestration. Atmos. Environ. 43, 2602–2611. https://doi.org/10.1016/j.atmosenv.2009.01.053.
Luo, Q., O'Leary, G., Cleverly, J., Eamus, D., 2018. Effectiveness of time of sowing and cultivar choice for managing climate change: wheat crop phenology and water use efficiency. Int. J. Biometeor. 62, 1049–1061. https://doi.org/10.1007/s00484-018-1508-4.
Lynch, A.H., Abramson, D., Görgen, K., Beringer, J., Uotila, P., 2007. Influence of savanna fire on Australian monsoon season precipitation and circulation as simulated using a distributed computing environment. Geophys. Res. Lett. 34, L20801. https://doi.org/10.1029/2007GL030879.
Ma, X., Huete, A., Cleverly, J., Eamus, D., Chevallier, F., Joiner, J., Poulter, B., Zhang, Y., Guanter, L., Meyer, W., Xie, Z., Ponce-Campos, G., 2016. Drought rapidly diminishes the large net CO_2 uptake in 2011 over semi-arid Australia. Sci. Rep. 6, 37747. https://doi.org/10.1038/srep37747.
Mallawaarachchi, T., Nauges, C., Sanders, O., Quiggin, J., 2017. State-contingent analysis of farmers' response to weather variability: irrigated dairy farming in the Murray Valley, Australia. Aust. J. Agr. Resour. Econ. 61, 36–55. https://doi.org/10.1111/1467-8489.12193.
Meier, E.A., Thorburn, P.J., Kragt, M.E., Dumbrell, N.P., Biggs, J.S., Hoyle, F.C., van Rees, H., 2017. Greenhouse gas abatement on southern Australian grains farms: biophysical potential and financial impacts. Agric. Syst. 155, 147–157. https://doi.org/10.1016/j.agsy.2017.04.012.
Moffat, A.M., Papale, D., Reichstein, M., Hollinger, D.Y., Richardson, A.D., Barr, A.G., Beckstein, C., Braswell, B.H., Churkina, G., Desai, A.R., Falge, E., Gove, J.H., Heimann, M., Hui, D.F., Jarvis, A.J., Kattge, J., Noormets, A., Stauch, V.J., 2007. Comprehensive comparison of gap-filling techniques for eddy covariance net carbon fluxes. Agric. For. Meteor. 147, 209–232.
Moinet, Y.G., Midwood, J.A., Hunt, E.J., Rumpel, C., Millard, P., Chabbi, A., 2019. Grassland management influences the response of soil respiration to drought. Agronomy 9. https://doi.org/10.3390/agronomy9030124.
Mudge, P.L., Wallace, D.F., Rutledge, S., Campbell, D.I., Schipper, L.A., Hosking, C.L., 2011. Carbon balance of an intensively grazed temperate pasture in two climatically contrasting years. Agric. Ecosyst. Environ. 144, 271–280. https://doi.org/10.1016/j.agee.2011.09.003.
Mueller, N.D., Rhines, A., Butler, E.E., Ray, D.K., Siebert, S., Holbrook, N.M., Huybers, P., 2017. Global relationships between cropland intensification and summer temperature extremes over the last 50 years. J. Clim. 30, 7505–7528. https://doi.org/10.1175/jcli-d-17-0096.1.
Murphy, B.P., Paron, P., Prior, L.D., Boggs, G.S., Franklin, D.C., Bowman, D., 2010. Using generalized autoregressive error models to understand fire-vegetation-soil feedbacks in a mulga-spinifex landscape mosaic. J. Biogeogr. 37, 2169–2182. https://doi.org/10.1111/j.1365-2699.2010.02359.x.
Orgill, S.E., Waters, C.M., Melville, G., Toole, I., Alemseged, Y., Smith, W., 2017. Sensitivity of soil organic carbon to grazing management in the semi-arid rangelands of south-eastern Australia. Rangeland J. 39, 153–167. https://doi.org/10.1071/rj16020.
Peng, L., Li, D., Sheffield, J., 2018. Drivers of variability in atmospheric evaporative demand: multiscale spectral analysis based on observations and physically based modeling. Water Resour. Res. 54, 3510–3529. https://doi.org/10.1029/2017WR022104.
Percival, D.B., Walden, A.T., 2000. Wavelet methods for time series analysis. Cambridge Series in Statistical and Probabilistic Mathematics. Cambridge University Press, New York, NY.
Porporato, A., Feng, X., Manzoni, S., Mau, Y., Parolari, A.J., Vico, G., 2015. Ecohydrological modeling in agroecosystems: examples and challenges. Water Resour. Res. 51, 5081–5099. https://doi.org/10.1002/2015WR017289.
Poulter, B., Frank, D., Ciais, P., Myneni, R.B., Andela, N., Bi, J., Broquet, G., Canadell, J.G., Chevallier, F., Liu, Y.Y., Running, S.W., Sitch, S., van der Werf, G.R., 2014. Contribution of semi-arid ecosystems to interannual variability of the global carbon cycle. Nature 509, 600–603. https://doi.org/10.1038/nature13376.
Rashid, M.A., Andersen, M.N., Wollenweber, B., Zhang, X.Y., Olesen, J.E., 2018. Acclimation to higher VPD and temperature minimized negative effects on assimilation and grain yield of wheat. Agric. For. Meteor. 248, 119–129. https://doi.org/10.1016/j.agrformet.2017.09.018.
Ratcliffe, J.L., Campbell, D.I., Clarkson, B.R., Wall, A.M., Schipper, L.A., 2019. Water table fluctuations control CO2 exchange in wet and dry bogs through different mechanisms. Sci. Total Environ. 655, 1037–1046. https://doi.org/10.1016/j.scitotenv.2018.11.151.
Raupach, M.R., Haverd, V., Briggs, P.R., 2013. Sensitivities of the Australian terrestrial water and carbon balances to climate change and variability. Agric. For. Meteor. 182–183, 277–291. https://doi.org/10.1016/j.agrformet.2013.06.017.
Regan, C.M., Connor, J.D., Segaran, R.R., Meyer, W.S., Bryan, B.A., Ostendorf, B., 2017. Climate change and the economics of biomass energy feedstocks in semi-arid agricultural landscapes: a spatially explicit real options analysis. J. Environ. Manage. 192, 171–183. https://doi.org/10.1016/j.jenvman.2017.01.049.
Renchon, A.A., Griebel, A., Metzen, D., Williams, C.A., Medlyn, B., Duursma, R.A., Barton, C.V.M., Maier, C., Boer, M.M., Isaac, P., Tissue, D., Resco de Dios, V., Pendall, E.,

2018. Upside-down fluxes down under: CO_2 net sink in winter and net source in summer in a temperate evergreen broadleaf forest. Biogeosciences 15, 3703–3716. https://doi.org/10.5194/bg-15-3703-2018.

Restrepo-Coupe, N., Huete, A., Davies, K., Cleverly, J., Beringer, J., Eamus, D., van Gorsel, E., Hutley, L.B., Meyer, W.S., 2016. MODIS vegetation products as proxies of photosynthetic potential along a gradient of meteorologically and biologically driven ecosystem productivity. Biogeosciences 13, 5587–5608. https://doi.org/10.5194/bg-13-5587-2016.

Rhif, M., Abbes, A.B., Farah, I.R., Martínez, B., Sang, Y., 2019. Wavelet transform application for/in non-stationary time-series analysis: a review. Appl. Sci 9. https://doi.org/10.3390/app9071345.

Rutledge, S., Mudge, P.L., Campbell, D.I., Woodward, S.L., Goodrich, J.P., Wall, A.M., Kirschbaum, M.U.F., Schipper, L.A., 2015. Carbon balance of an intensively grazed temperate dairy pasture over four years. Agric. Ecosyst. Environ. 206, 10–20. https://doi.org/10.1016/j.agee.2015.03.011.

Ryu, Y., Baldocchi, D.D., Ma, S., Hehn, T., 2008. Interannual variability of evapotranspiration and energy exchange over an annual grassland in California. J. Geophys. Res.: Atmos. 113, D09104.

Schaller, C., Göckede, M., Foken, T., 2017. Flux calculation of short turbulent events – comparison of three methods. Atmos. Meas. Tech. 10, 869–880. https://doi.org/10.5194/amt-10-869-2017.

Schipper, L.A., Petrie, O.J., O'Neill, T.A., Mudge, P.L., Liáng, L.L., Robinson, J.M., Arcus, V.L., 2019. Shifts in temperature response of soil respiration between adjacent irrigated and non-irrigated grazed pastures. Agric. Ecosyst. Environ. 285, 106620. https://doi.org/10.1016/j.agee.2019.106620.

Shao, C.L., Chen, J.Q., Li, L.H., Dong, G., Han, J.J., Abraha, M., John, R., 2017. Grazing effects on surface energy fluxes in a desert steppe on the Mongolian Plateau. Ecol. Appl. 27, 485–502. https://doi.org/10.1002/eap.1459.

Shi, H., Li, L., Eamus, D., Cleverly, J., Huete, A., Beringer, J., Yu, Q., van Gorsel, E., Hutley, L., 2014. Intrinsic climate dependency of ecosystem light and water-use-efficiencies across Australian biomes. Environ. Res. Lett. 9, 104002. https://doi.org/10.1088/1748-9326/9/10/104002.

Sloat, L.L., Gerber, J.S., Samberg, L.H., Smith, W.K., Herrero, M., Ferreira, L.G., Godde, C.M., West, P.C., 2018. Increasing importance of precipitation variability on global livestock grazing lands. Nat. Clim. Change. 8, 214–218. https://doi.org/10.1038/s41558-018-0081-5.

Statistics New Zealand, 2015. Total Area of Farms, 2013. Statistics New Zealand, New Zealand.

Stevens, R.M., Ewenz, C.M., Grigson, G., Conner, S.M., 2012. Water use by an irrigated almond orchard. Irrig. Sci. 30, 189–200. https://doi.org/10.1007/s00271-011-0270-8.

Stokes, C.J., Howden, S.M., Gifford, R.G., Meinke, H., Bange, M., McRae, D., Roth, G., Gaydon, D., Beecher, H.G., Reinke, R., Crimp, S., Park, S., Inman-Bamber, G., Webb, L., Barlow, E.W.R., Hennessy, K., Whetton, P.H., Booth, T.H., Kirschbaum, M.U.F., Battaglia, M., Stone, G., Cobon, D., Ash, A., McKeon, G., Miller, C.J., Jones, R.N., Hobday, A.J., Poloczanska, E.S., 2008. An overview of climate change adaptation in Australian primary industries: impacts, options and priorities. Report Prepared for the National Climate Change Research Strategy for Primary Industries. CSIRO, Canberra, ACT, Australia.

Stoy, P.C., Katul, G.G., Siqueira, M.B.S., Juang, J.Y., McCarthy, H.R., Kim, H.S., Oishi, A.C., Oren, R., 2005. Variability in net ecosystem exchange from hourly to inter-annual time scales at adjacent pine and hardwood forests: a wavelet analysis. Tree Physiol. 25, 887–902.

Stoy, P.C., Mauder, M., Foken, T., Marcolla, B., Boegh, E., Ibrom, A., Arain, M.A., Arneth, A., Aurela, M., Bernhofer, C., Cescatti, A., Dellwik, E., Duce, P., Gianelle, D., van Gorsel, E., Kiely, G., Knohl, A., Margolis, H., McCaughey, H., Merbold, L., Montagnani, L., Papale, D., Reichstein, M., Saunders, M., Serrano-Ortiz, P., Sottocornola, M., Spano, D., Vaccari, F., Varlagin, A., 2013. A data-driven analysis of energy balance closure across FLUXNET research sites: the role of landscape scale heterogeneity. Agric. For. Meteor. 171–172, 137–152. https://doi.org/10.1016/j.agrformet.2012.11.004.

Stull, R.B., 1988. An Introduction to Boundary Layer Meteorology. Atmospheric Sciences Library. Kluwer Academic Publishers, Boston, MA 666 pp.

Tallec, T., Béziat, P., Jarosz, N., Rivalland, V., Ceschia, E., 2013. Crops' water use efficiencies in temperate climate: comparison of stand, ecosystem and agronomical approaches. Agric. For. Meteor. 168, 69–81. https://doi.org/10.1016/j.agrformet.2012.07.008.

Tarin, T., Nolan, R.H., Medlyn, B.E., Cleverly, J., Eamus, D., 2020. Water-use efficiency in a semi-arid woodland with high rainfall variability. Global Change Biology 26 (2), 496–508. https://doi.org/10.1111/gcb.14866. In this issue.

Thompson, M.A., Campbell, D.I., Spronken-Smith, R.A., 1999. Evaporation from natural and modified raised peat bogs in New Zealand. Agric. For. Meteor. 95, 85–98. https://doi.org/10.1016/s0168-1923(99)00027-1.

Torrence, C., Compo, G.P., 1998. A practical guide to wavelet analysis. Bull. Amer. Meteor. Soc. 79, 61–78.

Ummenhofer, C.C., Xu, H., Twine, T.E., Girvetz, E.H., McCarthy, H.R., Chhetri, N., Nicholas, K.A., 2015. How climate change affects extremes in maize and wheat yield in two cropping regions. J. Clim. 28, 4653–4687. https://doi.org/10.1175/jcli-d-13-00326.1.

van Delden, L., Larsen, E., Rowlings, D., Scheer, C., Grace, P., 2016. Establishing turf grass increases soil greenhouse gas emissions in peri-urban environments. Urban Ecosyst. 1–14. https://doi.org/10.1007/s11252-016-0529-1.

van Dijk, A., Beck, H.E., Crosbie, R.S., de Jeu, R.A.M., Liu, Y.Y., Podger, G.M., Timbal, B., Viney, N.R., 2013. The millennium drought in southeast Australia (2001-2009): natural and human causes and implications for water resources, ecosystems, economy, and society. Water Resour. Res. 49, 1040–1057. https://doi.org/10.1002/wrcr.20123.

van Gorsel, E., Berni, J.A.J., Briggs, P., Cabello-Leblic, A., Chasmer, L., Cleugh, H.A., Hacker, J., Hantson, S., Haverd, V., Hughes, D., Hopkinson, C., Keith, H., Kljun, N., Leuning, R., Yebra, M., Zegelin, S., 2013. Primary and secondary effects of climate variability on net ecosystem carbon exchange in an evergreen *Eucalyptus* forest. Agric. For. Meteor 182–183, 248–256. https://doi.org/10.1016/j.agrformet.2013.04.027.

van Gorsel, E., Cleverly, J., Beringer, J., Cleugh, H., Eamus, D., Hutley, L.B., Isaac, P., Prober, S., 2018. Preface: Ozflux: a network for the study of ecosystem carbon and water dynamics across Australia and New Zealand. Biogeosciences 15, 349–352. https://doi.org/10.5194/bg-15-349-2018.

van Gorsel, E., Wolf, S., Cleverly, J., Isaac, P., Haverd, V., Ewenz, C., Arndt, S., Beringer, J., Resco de Dios, V., Evans, B.J., Griebel, A., Hutley, L.B., Keenan, T., Kljun, N., Macfarlane, C., Meyer, W.S., McHugh, I., Pendall, E., Prober, S.M., Silberstein, R., 2016. Carbon uptake and water use in woodlands and forests in southern Australia during an extreme heat wave event in the "Angry Summer" of 2012/2013. Biogeosciences 13, 5947–5964. https://doi.org/10.5194/bg-13-5947-2016.

van Heerwaarden, C.C., Teuling, A.J., 2014. Disentangling the response of forest and grassland energy exchange to heatwaves under idealized land-atmosphere coupling. Biogeosciences 11, 6159–6171. https://doi.org/10.5194/bg-11-6159-2014.

Vote, C., Hall, A., Charlton, P., 2015. Carbon dioxide, water and energy fluxes of irrigated broad-acre crops in an Australian semi-arid climate zone. Environ Earth Sci 73, 449–465. https://doi.org/10.1007/s12665-014-3547-4.

Wagle, P., Gowda, P.H., Anapalli, S.S., Reddy, K.N., Northup, B.K., 2017a. Growing season variability in carbon dioxide exchange of irrigated and rainfed soybean in the southern United States. Sci. Total Environ. 593, 263–273. https://doi.org/10.1016/j.scitotenv.2017.03.163.

Wagle, P., Xiao, X.M., Gowda, P., Basara, J., Brunsell, N., Steiner, J., Anup, K.C., 2017b. Analysis and estimation of tallgrass prairie evapotranspiration in the central United States. Agric. For. Meteor. 232, 35–47. https://doi.org/10.1016/j.agrformet.2016.08.005.

Waldo, S., Chi, J., Pressley, S.N., O'Keeffe, P., Pan, W.L., Brooks, E.S., Huggins, D.R., Stöckle, C.O., Lamb, B.K., 2016. Assessing carbon dynamics at high and low rainfall agricultural sites in the inland Pacific Northwest US using the eddy covariance method. Agric. For. Meteor. 218–219, 25–36. https://doi.org/10.1016/j.agrformet.2015.11.018.

Wang, L., Liu, H.Z., Bernhofer, C., 2017. Response of carbon dioxide exchange to grazing intensity over typical steppes in a semi-arid area of Inner Mongolia. Theor. Appl. Climatol. 128, 719–730. https://doi.org/10.1007/s00704-016-1736-7.

Waters, C.M., Orgill, S.E., Melville, G.J., Toole, I.D., Smith, W.J., 2017. Management of grazing intensity in the semi-arid rangelands of Southern Australia: effects on soil and biodiversity. Land Degrad. Dev. 28, 1363–1375. https://doi.org/10.1002/ldr.2602.

Webb, J.R., Santos, I.R., Maher, D.T., Macdonald, B., Robson, B., Isaac, P., McHugh, I., 2018. Terrestrial versus aquatic carbon fluxes in a subtropical agricultural floodplain over an annual cycle. Agric. For. Meteor. 260-261, 262–272. https://doi.org/10.1016/j.agrformet.2018.06.015.

Whitehead, D., Schipper, L.A., Pronger, J., Moinet, G.Y.K., Mudge, P.L., Calvelo Pereira, R., Kirschbaum, M.U.F., McNally, S.R., Beare, M.H., Camps-Arbestain, M., 2018. Management practices to reduce losses or increase soil carbon stocks in temperate grazed grasslands: New Zealand as a case study. Agric. Ecosyst. Environ. 265, 432–443. https://doi.org/10.1016/j.agee.2018.06.022.

Whitley, R.J., Macinnis-Ng, C.M.O., Hutley, L.B., Beringer, J., Zeppel, M., Williams, M., Taylor, D., Eamus, D., 2011. Is productivity of mesic savannas light limited or water limited? Results of a simulation study. Glob. Change Biol 17, 3130–3149. https://doi.org/10.1111/j.1365-2486.2011.02425.x.

Williams, J., Hook, R.A., Hamblin, A., 2002. Agro-ecological Regions of Australia: Methodologies for their Derivation and key Issues in Resource Management. CSIRO Land and Water, Canberra, ACT, Australia.

Xie, Z., Huete, A., Cleverly, J., Phinn, S., McDonald-Madden, E., Cao, Y., Qin, F., 2019. Multi-climate mode interactions drive hydrological and vegetation responses to hydroclimatic extremes in Australia. Remote Sens. Environ. 231, 111270. https://doi.org/10.1016/j.rse.2019.111270.

Yang, Z., Dominguez, F., Zeng, X.B., Hu, H.C., Gupta, H., Yang, B., 2017. Impact of irrigation over the California Central Valley on regional climate. J. Hydrometeor. 18, 1341–1357.

Zeeman, M.J., Hiller, R., Gilgen, A.K., Michna, P., Pluss, P., Buchmann, N., Eugster, W., 2010. Management and climate impacts on net CO2 fluxes and carbon budgets of three grasslands along an elevational gradient in Switzerland. Agric. For. Meteor. 150, 519–530. https://doi.org/10.1016/j.agrformet.2010.01.011.

Zhang, Y.Q., Chiew, F.H.S., Pena-Arancibia, J., Sun, F.B., Li, H.X., Leuning, R., 2017. Global variation of transpiration and soil evaporation and the role of their major climate drivers. J. Geophys. Res.: Atmos. 122, 6868–6881. https://doi.org/10.1002/2017jd027025.

Zhou, Y.T., Xiao, X.M., Wagle, P., Bajgain, R., Mahan, H., Basara, J.B., Dong, J.W., Qin, Y.W., Zhang, G.L., Luo, Y.Q., Gowda, P.H., Neel, J.P.S., Starks, P.J., Steiner, J.L., 2017. Examining the short-term impacts of diverse management practices on plant phenology and carbon fluxes of Old World bluestems pasture. Agric. For. Meteor. 237, 60–70. https://doi.org/10.1016/j.agrformet.2017.01.018.

Zscheischler, J., Fatichi, S., Wolf, S., Blanken, P.D., Bohrer, G., Clark, K., Desai, A.R., Hollinger, D., Keenan, T., Novick, K.A., Seneviratne, S.I., 2016. Short-term favorable weather conditions are an important control of interannual variability in carbon and water fluxes. J. Geophys. Res.: Biogeosci. 121, 2186–2198. https://doi.org/10.1002/2016JG003503.